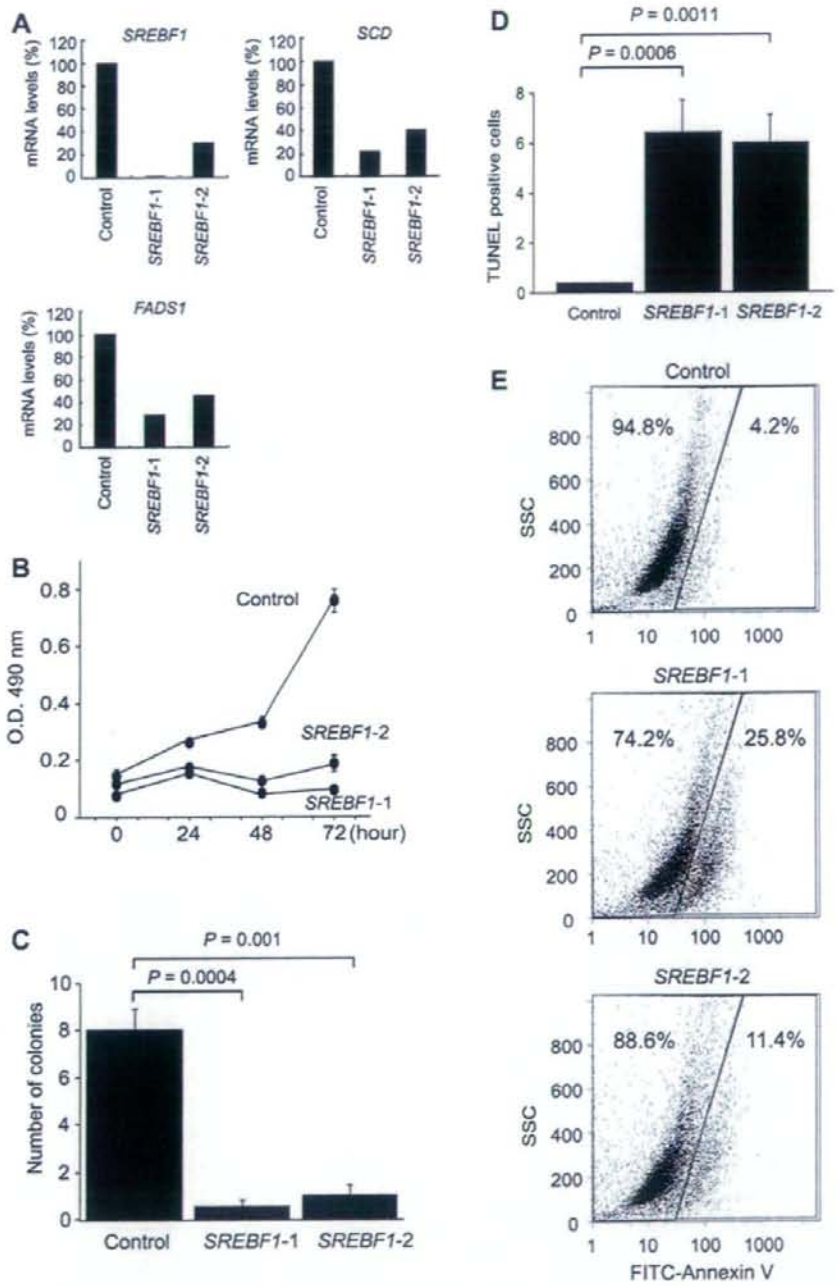

Fig. 2. (A) Effect of RNA interference targeting *SREBF1* in HuH7 cells. Expression levels of *SREBF1* mRNA were reduced by si-RNAs targeting different exons in *SREBF1*. Transcripts of *FADS1* and *SCD* were also down-regulated, showing transcriptional deactivation of the lipogenesis pathway. (B) Cell proliferation assay. Deactivation of the lipogenesis pathway severely reduced cell growth in HuH7 cells. (C) Soft agar assay. Deactivation of the lipogenesis pathway inhibited anchorage independent cell growth in HuH7 cells. (D) TUNEL assay. Deactivation of the lipogenesis pathway significantly increased the number of TUNEL-positive cells in HuH7 cells. (E) Annexin V staining evaluated by flow cytometer. Deactivation of the lipogenesis pathway significantly increased the number of annexin V positive cells in HuH7 cells.

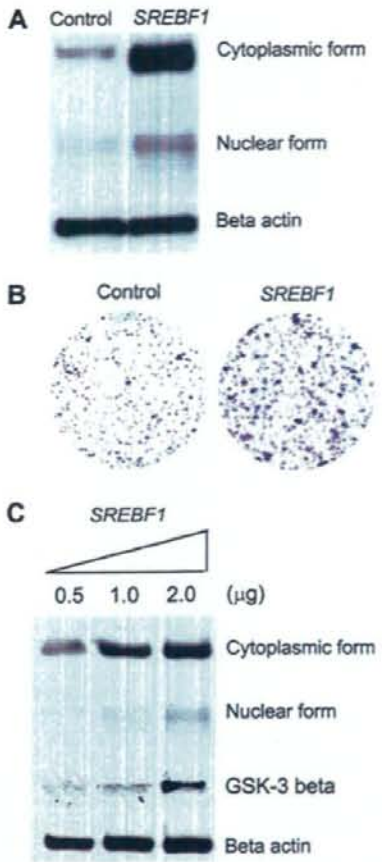

Fig. 3. (A) Western blot analysis of *SREBF1* protein expression in HuH7 cells transfected with control pCMV7 plasmids or pCMV7-*SREBF1c* plasmids. Both cytoplasmic and nuclear forms of *SREBF1* protein expression were increased by pCMV7-*SREBF1c* overexpression. (B) Focus assay of HuH7 cells transfected with control pCMV7 plasmids or pCMV7-*SREBF1c* plasmids. (C) Western blot analysis of *SREBF1* and phospho-GSK-3β protein expression in HuH7 cells transfected with indicated amounts of pCMV7-*SREBF1c* plasmids.

significance (HR, 3.7; 95% CI, 1.0–13.7; $P = 0.05$; Table 2).

4. Discussion

Using large-scale gene expression profiling, we have shown that the lipogenesis pathway is transcriptionally activated in HCC. Our SAGE profiles will be available on our homepage (http://www.intmedkanazawa.jp/) and will be submitted to the Gene Expression Omnibus (http://www.ncbi.nlm.nih.gov/geo/).

We found that the levels of expression of *FADS1*, *SCD*, and *FASN* were each correlated with those of *SREBF1*, suggesting that *SREBF1* is one of the main factors involved in the activation of lipogenesis in HCC. Activation of growth signaling pathways, such as the PI 3-kinase and mitogen-activated protein kinase pathways, has been shown to induce up-regulation of *SREBF1* in prostate and breast cancer cells [33,34]. We have observed induction of *SREBF1* protein expression by IGF2 in HuH7 cells (data not shown). Furthermore, we have identified that *SREBF1* overexpression results in the activation of cell proliferation and PI 3-kinase signaling, whereas expression inhibition of *SREBF1* abrogated the IGF2 induced cell proliferation. Although detailed mechanisms should be clarified in future, our results suggest that *SREBF1* is a key component of PI 3-kinase signaling in HCC.

SREBF1 is induced by alcohol [35], insulin, and fat [30,36], and plays a central role in the mechanism of hepatic steatosis [37]. Interestingly, these *SREBF1* inducers are risk factors for HCC [12,13,38,14]. Strikingly, two recent studies have shown that HBV and HCV infection may also induce hepatic steatosis through activation of *SREBF1* [39,40]. Furthermore, a recent report revealed the activation of *SREBF1* signaling in cancer by hypoxia [41]. Thus, these pathologic conditions such as chronic viral hepatitis, alcohol abuse, obesity, diabetes, and local hypoxia may up-regulate the expression of *SREBF1*, which, in turn, may contribute to an increased risk of hepatocarcinogenesis. Transgenic mice overexpressing *SREBF1* in the liver exhibited hepatic steatosis and hepatomegaly, suggesting the role of *SREBF1* on lipid metabolism and cell proliferation. However, it should be noted that no transgenic mice overexpressing *SREBF1* have been reported to have the risk of HCC development thus far. Interestingly, a recent report indicated that HCV core transgenic mice known to develop HCC showed coordinated activation of lipogenic pathway genes and *SREBF1* [42]. Although further studies are clearly required, we speculate that the activation of *SREBF1* may contribute to promote the development of HCC in already-initiated hepatocytes but not in normal hepatocytes.

Recently, Yahagi et al. reported the activation of lipogenic enzyme related genes in HCC [31]. In that paper, the authors suggested that *SREBF1* expression was not correlated with the expression of other lipogenic genes by Northern blotting, inconsistent with our current data. One possible explanation of these discrepancies might be the different methods for quantitation of mRNA, and we believe that real-time RT-PCR method used in our study would be more accurate. In addition, we evaluated the expression of *SREBF1* and lipogenic genes using more samples (a total of 44 liver and HCC tissues) than Yahagi et al did (10 HCC tissues). Furthermore, a recent paper indicated the coordinated activation of *SREBF1* and lipogenic genes in HCC

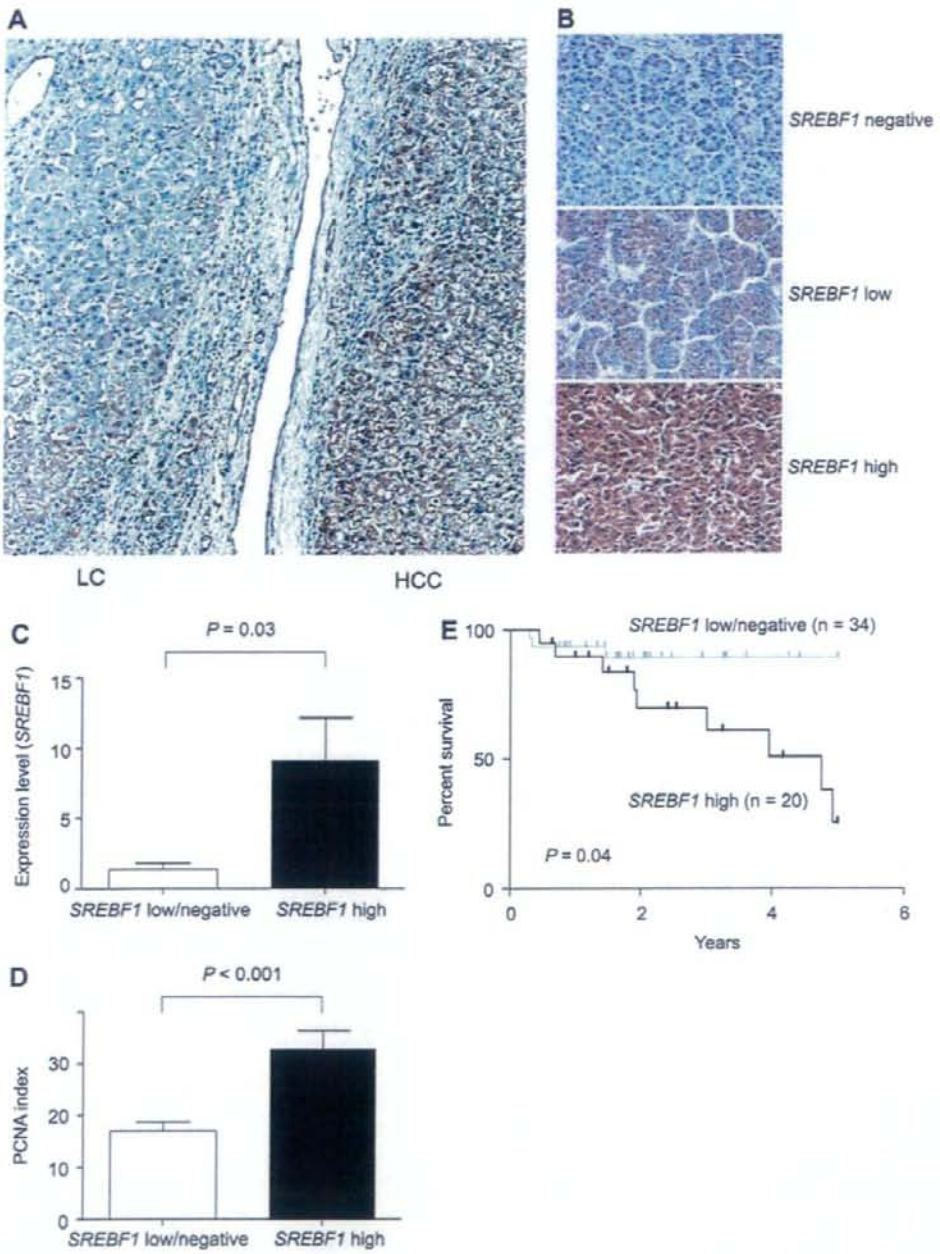

Fig. 4. (A) A photomicrograph of an HCC with adjacent non-cancerous cirrhotic liver stained with anti-*SREBF1* antibodies. (B) Representative photomicrographs of *SREBF1*-negative-, *SREBF1*-low-, and *SREBF1*-high-HCC tissues stained with anti- *SREBF1* antibodies. (C) *SREBF1* gene expression by real-time RT-PCR according to protein expression status assessed by IHC. *SREBF1* was highly expressed in *SREBF1*-high HCC ($P = 0.03$). (D) SREBF1 expression and cell proliferation in HCC. PCNA indexes in *SREBF1*-high HCC were higher than those in *SREBF1*-low/-negative HCC with statistical significance ($P < 0.001$). (E) Kaplan–Meier plots of 54 HCC patients analyzed by immunohistochemistry. The differences between *SREBF1*-high and -low/-negative HCC were analyzed by log-rank test.

developed in the liver of HCV core transgenic mice [42], strongly support our data. Although further studies using large numbers of HCC tissues may be required, these data suggest that the lipogenic gene activation seems to be mediated, at least in part, by *SREBF1* expression in HCC.

Table 2
Univariate Cox regression analysis of survival relative to *SREBF1* protein expression and clinicopathological parameters.

Variables (n)	HR (95% CI)	P-value
SREBF1 and mortality ($n = 54$)		
Tumor size		
<3 cm ($n = 37$)	1	
⩾3 cm ($n = 17$)	2.2 (0.6–8.3)	0.2
pTNM stage		
I, II ($n = 45$)	1	
III, IV ($n = 9$)	2.0 (0.4–9.4)	0.4
Serum AFP		
<20 ng/ml ($n = 35$)	1	
⩾20 ng/ml (n = 19)	1.5 (0.4–5.4)	0.5
SREBF1		
Low ($n = 34$)	1	
High ($n = 20$)	3.7 (1.0–13.7)	0.05

Because the majority of our HCC patients analyzed had Child–Pugh class A scores and about 70% had tumors less than 3 cm in diameter, all were expected to have a good prognosis. Indeed, patient survival in this cohort was not segregated by tumor size or pTNM stage (Table 2). Although the sample size was relatively small, we found that enhanced expression of *SREBF1* was a prognostic factor for mortality in HCC possibly due to the highly proliferative nature. Activation of lipogenesis pathways, as shown by overexpression of *FASN*, has been found to correlate with high mortality in breast, prostate, and lung cancer [43], suggesting that activation of lipogenesis may be a fundamental characteristic of cancer with poor prognosis. Thus, *SREBF1* expression may be a good biomarker for HCC classification, a finding that should be validated in a large scale cohort. Because deactivation of the lipogenesis pathway by inhibition of *SREBF1* gene expression could inhibit HCC cell growth *in vitro*, *SREBF1* may be a good target for pharmaceutical intervention in these tumors.

In conclusion, our genome-wide gene expression profiling analyses found that the lipogenesis pathway was activated in a subset of HCC. *SREBF1*, which activates the lipogenesis pathway, may be a good biomarker for HCC prognosis and may be a good target for therapeutic intervention.

Acknowledgements

We are grateful to the members of The Liver Disease Center at Kanazawa University Hospital for providing data of human liver tissue samples. We would also like to thank Dr. Hitoshi Shimano for providing invaluable reagents.

Appendix A. Supplementary data

Supplementary data associated with this article can be found, in the online version, at doi:10.1016/j.jhep.2008.07.036.

References

[1] El-Serag HB, Mason AC. Rising incidence of hepatocellular carcinoma in the United States. N Engl J Med 1999;340:745–750.
[2] Bosch FX, Ribes J, Diaz M, Cleries R. Primary liver cancer: worldwide incidence and trends. Gastroenterology 2004;127:S5–S16.
[3] Wang XW, Hussain SP, Huo TI, Wu CG, Forgues M, Hofseth LJ, et al. Molecular pathogenesis of human hepatocellular carcinoma. Toxicology 2002;181-182:43–47.
[4] Yamashita T, Kaneko S, Hashimoto S, Sato T, Nagai S, Toyoda N, et al. Serial analysis of gene expression in chronic hepatitis C and hepatocellular carcinoma. Biochem Biophys Res Commun 2001;282:647–654.
[5] Shirota Y, Kaneko S, Honda M, Kawai HF, Kobayashi K. Identification of differentially expressed genes in hepatocellular carcinoma with cDNA microarrays. Hepatology 2001;33:832–840.
[6] Okabe H, Satoh S, Kato T, Kitahara O, Yanagawa R, Yamaoka Y, et al. Genome-wide analysis of gene expression in human hepatocellular carcinomas using cDNA microarray: identification of genes involved in viral carcinogenesis and tumor progression. Cancer Res 2001;61:2129–2137.
[7] Xu XR, Huang J, Xu ZG, Qian BZ, Zhu ZD, Yan Q, et al. Insight into hepatocellular carcinogenesis at transcriptome level by comparing gene expression profiles of hepatocellular carcinoma with those of corresponding noncancerous liver. Proc Natl Acad Sci USA 2001;98:15089–15094.
[8] Iizuka N, Oka M, Yamada-Okabe H, Mori N, Tamesa T, Okada T, et al. Comparison of gene expression profiles between hepatitis B virus- and hepatitis C virus-infected hepatocellular carcinoma by oligonucleotide microarray data on the basis of a supervised learning method. Cancer Res 2002;62:3939–3944.
[9] Thorgeirsson SS, Grisham JW. Molecular pathogenesis of human hepatocellular carcinoma. Nat Genet 2002;31:339–346.
[10] Lee JS, Thorgeirsson SS. Genome-scale profiling of gene expression in hepatocellular carcinoma: classification, survival prediction, and identification of therapeutic targets. Gastroenterology 2004;127:S51–S55.
[11] Suriawinata A, Xu R. An update on the molecular genetics of hepatocellular carcinoma. Semin Liver Dis 2004;24:77–88.
[12] El-Serag HB, Tran T, Everhart JE. Diabetes increases the risk of chronic liver disease and hepatocellular carcinoma. Gastroenterology 2004;126:460–468.
[13] Hassan MM, Hwang LY, Hatten CJ, Swaim M, Li D, Abbruzzese JL, et al. Risk factors for hepatocellular carcinoma: synergism of alcohol with viral hepatitis and diabetes mellitus. Hepatology 2002;36:1206–1213.
[14] Ohata K, Hamasaki K, Toriyama K, Matsumoto K, Saeki A, Yanagi K, et al. Hepatic steatosis is a risk factor for hepatocellular carcinoma in patients with chronic hepatitis C virus infection. Cancer 2003;97:3036–3043.
[15] Calle EE, Rodriguez C, Walker-Thurmond K, Thun MJ. Overweight, obesity, and mortality from cancer in a prospectively studied cohort of US adults. N Engl J Med 2003;348:1625–1638.
[16] Walsh MJ, Vanags DM, Clouston AD, Richardson MM, Purdie DM, Jonsson JR, et al. Steatosis and liver cell apoptosis in chronic hepatitis C: a mechanism for increased liver injury. Hepatology 2004;39:1230–1238.

[17] Powell EE, Jonsson JR, Clouston AD. Steatosis: co-factor in other liver diseases. Hepatology 2005;42:5–13.
[18] Velculescu VE, Zhang L, Vogelstein B, Kinzler KW. Serial analysis of gene expression. Science 1995;270:484–487.
[19] Yamashita T, Hashimoto S, Kaneko S, Nagai S, Toyoda N, Suzuki T, et al. Comprehensive gene expression profile of a normal human liver. Biochem Biophys Res Commun 2000;269:110–116.
[20] Desmet VJ, Gerber M, Hoofnagle JH, Manns M, Scheuer PJ. Classification of chronic hepatitis: diagnosis, grading and staging. Hepatology 1994;19:1513–1520.
[21] Polyak K, Xia Y, Zweier JL, Kinzler KW, Vogelstein B. A model for p53-induced apoptosis. Nature 1997;389:300–305.
[22] Yokoyama C, Wang X, Briggs MR, Admon A, Wu J, Hua X, et al. SREBP-1, a basic-helix–loop-helix–leucine zipper protein that controls transcription of the low density lipoprotein receptor gene. Cell 1993;75:187–197.
[23] Wang HC, Chang WT, Chang WW, Wu HC, Huang W, Lei HY, et al. Hepatitis B virus pre-S2 mutant upregulates cyclin A expression and induces nodular proliferation of hepatocytes. Hepatology 2005;41:761–770.
[24] Takeba Y, Kumai T, Matsumoto N, Nakaya S, Tsuzuki Y, Yanagida Y, et al. Irinotecan activates p53 with its active metabolite, resulting in human hepatocellular carcinoma apoptosis. J Pharmacol Sci 2007;104:232–242.
[25] Closset J, Van de Stadt J, Delhaye M, El Nakadi I, Lambilliotte JP, Gelin M. Hepatocellular carcinoma: surgical treatment and prognostic variables in 56 patients. Hepatogastroenterology 1999;46:2914–2918.
[26] Arsura M, Cavin LG, Calvisi DF, Thorgeirsson SS, Eferl R, Ricci R, et al. Nuclear factor-kappaB and liver carcinogenesis. Cancer Lett 2005;229:157–169.
[27] Calvisi DF, Thorgeirsson SS. Molecular mechanisms of hepatocarcinogenesis in transgenic mouse models of liver cancer. Toxicol Pathol 2005;33:181–184.
[28] Eferl R, Ricci R, Kenner L, Zenz R, David JP, Rath M, et al. Liver tumor development. c-Jun antagonizes the proapoptotic activity of p53. Cell 2003;112:181–192.
[29] Xu L, Hui L, Wang S, Gong J, Jin Y, Wang Y, et al. Expression profiling suggested a regulatory role of liver-enriched transcription factors in human hepatocellular carcinoma. Cancer Res 2001;61:3176–3181.
[30] Horton JD, Goldstein JL, Brown MS. SREBPs: activators of the complete program of cholesterol and fatty acid synthesis in the liver. J Clin Invest 2002;109:1125–1131.
[31] Yahagi N, Shimano H, Hasegawa K, Ohashi K, Matsuzaka T, Najima Y, et al. Co-ordinate activation of lipogenic enzymes in hepatocellular carcinoma. Eur J Cancer 2005;41:1316–1322.
[32] Kawaguchi K, Honda M, Yamashita T, Shirota Y, Kaneko S. Differential gene alteration among hepatoma cell lines demonstrated by cDNA microarray-based comparative genomic hybridization. Biochem Biophys Res Commun 2005;329:370–380.
[33] Van de Sande T, De Schrijver E, Heyns W, Verhoeven G, Swinnen JV. Role of the phosphatidylinositol 3′-kinase/PTEN/Akt kinase pathway in the overexpression of fatty acid synthase in LNCaP prostate cancer cells. Cancer Res 2002;62:642–646.
[34] Yang YA, Han WF, Morin PJ, Chrest FJ, Pizer ES. Activation of fatty acid synthesis during neoplastic transformation: role of mitogen-activated protein kinase and phosphatidylinositol 3-kinase. Exp Cell Res 2002;279:80–90.
[35] You M, Fischer M, Deeg MA, Crabb DW. Ethanol induces fatty acid synthesis pathways by activation of sterol regulatory element-binding protein (SREBP). J Biol Chem 2002;277:29342–29347.
[36] Muller-Wieland D, Kotzka J. SREBP-1: gene regulatory key to syndrome X? Ann NY Acad Sci 2002;967:19–27.
[37] Sekiya M, Yahagi N, Matsuzaka T, Najima Y, Nakakuki M, Nagai R, et al. Polyunsaturated fatty acids ameliorate hepatic steatosis in obese mice by SREBP-1 suppression. Hepatology 2003;38:1529–1539.
[38] Marrero JA, Fontana RJ, Su GL, Conjeevaram HS, Emick DM, Lok AS. NAFLD may be a common underlying liver disease in patients with hepatocellular carcinoma in the United States. Hepatology 2002;36:1349–1354.
[39] Kim KH, Shin HJ, Kim K, Choi HM, Rhee SH, Moon HB, et al. Hepatitis B virus X protein induces hepatic steatosis via transcriptional activation of SREBP1 and PPARgamma. Gastroenterology 2007;132:1955–1967.
[40] Waris G, Felmlee DJ, Negro F, Siddiqui A. Hepatitis C virus induces proteolytic cleavage of sterol regulatory element binding proteins and stimulates their phosphorylation via oxidative stress. J Virol 2007;81:8122–8130.
[41] Furuta E, Pai SK, Zhan R, Bandyopadhyay S, Watabe M, Mo YY, et al. Fatty acid synthase gene is up-regulated by hypoxia via activation of Akt and sterol regulatory element binding protein-1. Cancer Res 2008;68:1003–1011.
[42] Tanaka N, Moriya K, Kiyosawa K, Koike K, Gonzalez FJ, Aoyama T. PPARalpha activation is essential for HCV core protein-induced hepatic steatosis and hepatocellular carcinoma in mice. J Clin Invest 2008;118:683–694.
[43] Kuhajda FP. Fatty acid synthase and cancer: new application of an old pathway. Cancer Res 2006;66:5977–5980.

ELSEVIER

Journal of Hepatology 49 (2008) 946–954

Journal of Hepatology

www.elsevier.com/locate/jhep

Expression of multidrug resistance-associated protein 3 and cytotoxic T cell responses in patients with hepatocellular carcinoma☆

Eishiro Mizukoshi, Masao Honda, Kuniaki Arai, Tatsuya Yamashita, Yasunari Nakamoto, Shuichi Kaneko*

Department of Gastroenterology, Graduate School of Medicine, Kanazawa University, Kanazawa, Ishikawa 920-8641, Japan

***Background/Aims*: Multidrug resistance-associated protein 3 (MRP3) is a carrier-type transport protein belonging to the ABC transporters. It is expressed in normal tissues, and enhanced expression in many cancers has been reported. In this study, we investigated the usefulness of MRP3 as a target antigen in immunotherapy for hepatocellular carcinoma (HCC).**

***Methods*: The MRP3 expression level in HCC tissue was measured by quantitative PCR. MRP3-specific T cell responses were investigated by several immunological techniques using peripheral blood mononuclear cells or tumor-infiltrating lymphocytes.**

***Results*: The MRP3 expression level in HCC tissue was significantly higher than that in non-cancerous tissue ($P < 0.05$). MRP3-specific cytotoxic T cells (CTLs) could be induced regardless of liver function, the presence or absence of HCV infection, the blood AFP level, and the stage of HCC. The CTLs showed cytotoxicity against HCC cells overexpressing MRP3. A negative correlation was present between the MRP3 expression level in HCC tissue and the frequency of MRP3-specific CTLs. The frequency of MRP3-specific CTLs increased after HCC treatment, such as transcatheter arterial embolization and radiofrequency ablation.**

***Conclusions*: Our study demonstrates that MRP3 is a potential candidate for tumor antigen with strong immunogenicity in HCC immunotherapy.**

***Keywords*: Immune response; CD8; HLA-A24; Hepatitis; Cancer**

1. Introduction

Hepatocellular carcinoma (HCC) is treatable by hepatectomy or percutaneous ablation when the lesion is localized to some extent, and radical therapeutic effects can be obtained when the resection or cauterization with a safety margin can be performed [1,2]. However, active hepatitis and cirrhosis in the surrounding non-tumor liver tissues exhibit high carcinogenetic potentials to develop *de novo* HCC, and therefore, the recurrence rate of HCC after treatment is very high [3,4].

To protect against recurrence, tumor antigen-specific immunotherapy is an attractive strategy. For the development of HCC-specific immunotherapy and analysis of immune responses to the treatment, the identification of HCC-specific tumor antigens or their antigenic epitopes is necessary. However, only a few HCC-specific tumor antigens and their antigenic epitopes have been identified [5–10].

MRP3 is a carrier-type transport protein belonging to the ABC transporters that transport substances against

Received 11 January 2008; received in revised form 23 April 2008; accepted 7 May 2008; available online 5 June 2008

Associate Editor: V. Barnaba

☆ The authors declare that they do not have anything to disclose regarding funding from industries or conflict of interest with respect to this manuscript.

* Corresponding author. Tel.: +81 76 265 2230; fax: +81 76 234 4250.

E-mail address: skaneko@m-kanazawa.jp (S. Kaneko).

Abbreviations: HLA, human leukocyte antigen; IFN, interferon; PBMC, peripheral blood mononuclear cell; TIL, tumor-infiltrating lymphocytes; HCV, hepatitis C virus; ELISPOT, enzyme linked immunospot.

0168-8278/$34.00 © 2008 European Association for the Study of the Liver. Published by Elsevier B.V. All rights reserved.
doi:10.1016/j.jhep.2008.05.012

the concentration gradient in an ATP energy-dependent manner [11]. It is expressed at a high level in the small and large intestine, pancreas, placenta, and adrenal cortex [12], and recent studies have reported that its expression is enhanced in various cancer cells [13–15]. Yamada et al. demonstrated that MRP3 was a tumor rejection antigen recognized by cytotoxic T cells (CTLs), using lymphocytes infiltrating into lung adenocarcinoma, and identified its CTL epitope [13]. These reports suggest that MRP3 may be useful as a target antigen in HCC immunotherapy. However, the MRP3 expression level in HCC tissue has been controversial [16,17], and the association between the expression level and the degree of the immune response to MRP3 in HCC patients has not been clarified.

In this study, we measured the MRP3 expression level in various hematoma cell lines and HCC tissues in HCC patients, and analyzed immune responses to MRP3 using peripheral blood mononuclear cells (PBMCs) and tumor-infiltrating lymphocytes (TILs) to investigate the usefulness of MRP3 in HCC immunotherapy.

2. Materials and methods

2.1. Patients

This study examined 103 HLA-A24-positive patients with HCC (Table 1). All subjects were negative for Abs to human immunodeficiency virus (HIV), and gave written informed consent to participate in this study in accordance with the Helsinki declaration. The diagnosis of HCC was histologically confirmed by taking US-guided needle biopsy specimens in 35 cases, surgical resection in 13 cases, and autopsy in 4 cases. For the remaining 51 patients, the diagnosis was based on typical hypervascular tumor staining on angiography in addition to typical findings, which showed hyperattenuated areas in the early phase and hypoattenuation in the late phase on dynamic CT [18]. Eleven healthy blood donors with HLA-A24, who did not have a history of cancer and were negative for HBsAg and anti-HCVAb, served as controls.

2.2. Laboratory and virologic testing

Blood samples were tested for HBsAg and HCVAb by commercial immunoassays (Fuji Rebio, Tokyo, Japan). HLA-based typing of PBMC from patients and normal donors was performed as previously described [10].

The serum AFP level was measured by enzyme immunoassay (AxSYM AFP, Abbott Japan, Tokyo, Japan) and the pathological grading of tumor cell differentiation was assessed according to the general rules for the clinical and pathologic study of primary liver cancer [19]. The severity of liver disease (stage of fibrosis) was evaluated according to the criteria of Desmet et al. [20] using biopsy specimens of liver tissue, where F4 was defined as cirrhosis.

2.3. Cell lines

Eight human hepatoma cell lines: HepG2, Alex, Huh6, HLE, HLF, Hep3B, SKHep1, and Huh7, were cultured in DMEM (Gibco, Grand Island, NY, USA) with 10% fetal calf serum (FCS) (Gibco, Grand Island, NY, USA). The HLA-A*2402 gene-transfected C1R cell line (C1R-A24) [21] was cultured in RPMI 1640 medium containing 10% FCS and 500 μg/ml of hygromycin B (Sigma, St. Louis, MO, USA), and K562 was cultured in RPMI 1640 medium containing 10% FCS.

2.4. Quantitative real time detection (RTD)-PCR

We performed quantitative RTD-PCR using TaqMan Universal Master Mix (PE Applied Biosystems, Foster City, CA, USA). Primer pairs and probes for MRP3 and β-actin were obtained from TaqMan assay reagents library. Total RNA was isolated from cell lines and liver tissue samples using an RNA extraction kit (Micro RNA Extraction Kit, Stratagene, La Jolla, CA, USA). We reverse-transcribed 1 μg of isolated RNA to cDNA using SuperScript® II RT (Invitrogen, Carlsbad, CA, USA) according to the manufacturer's instructions, and the resultant cDNA was amplified with appropriate TaqMan assay reagents as previously described [22].

2.5. Preparation of PBMCs and TILs

PBMCs and TILs were isolated as previously described [9]. Fresh PBMCs were used for the CTL induction, and the remaining PBMCs and TILs were resuspended in RPMI 1640 medium containing 80% FCS and 10% dimethyl sulfoxide and cryopreserved until used. In patients with treatment, PBMCs were obtained before and 2–4 weeks after the treatment.

2.6. CTL induction and cytotoxicity assay

Peptides $MRP3_{503}$, $MRP3_{692}$, and $MRP3_{765}$, which were identified to contain a HLA-A24 restricted CTL epitope [13], were used for the induction of MRP3-specific T cells (Table 2). Peptides were synthesized at Mimotope (Melbourne, Australia) and Sumitomo Pharmaceuticals (Osaka, Japan). They were identified using mass spectrometry, and their purities were determined to be >80% by analytical HPLC. CTLs were expanded from PBMCs as previously described [23]. Briefly, four hundred thousand cells per well were stimulated with synthetic peptides at 10 μg/ml, 10 ng/ml rIL-7 and 100 pg/ml rIL-12 (Sigma, St. Louis, Mo) in RPMI 1640 supplemented with 10% heat inactivated human AB serum, 100 U/ml penicillin and 100 μg/ml streptomycin. The cultures were re-stimulated with 10 μg/ml peptide, 20 U/ml rIL-2 (Sigma, St. Louis, MO) and 10^5 mytomicin C treated autologous PBMCs on days 7 and 14. On days 3, 10 and 17, 100 μl of RPMI with 10% human AB serum and 10 U/ml rIL-2 (final concentration) was added to each well.

C1R-A24 cells and human hepatoma cell lines were used as target cells. Cytotoxicity assays were performed in at least 10 HCC patients for each peptide as previously described [10]. Spontaneous release

Table 1
Characteristics of the patients studied

Clinical diagnosis	No. of patients	Sex M/F	Age (yr) Mean ± SD	ALT (IU/L) Mean ± SD	AFP (ng/ml) mean ± SD	Etiology (B/C/B + C/Others)	Child Pugh (A/B/C)	Diff. degree[a] (Wel/Mod/Por/ND)	Tumor size[b] (Large/Small)	Tumor multiplicity (Multiple/Solitary)	Vascular Invasion (+/−)	TNM stage (I/II/IIIA/IIIB/IIIC/IV)
HCC patients	103	79/24	63 ± 10	65 ± 37	3155 ± 15946	19/73/2/9	61/39/3	17/31/4/51	79/24	73/30	30/73	24/51/16/1/3/8
Normal donors	11	8/3	35 ± 2	ND	ND	ND	ND	ND	ND	ND	ND	ND

[a] Histological degree of HCC: wel: well-differentiated, mod: moderately differentiated, por: poorly differentiated, ND: not determined.
[b] Tumor size was divided into either 'small' (≤2 cm) or 'large' (>2 cm).

Table 2
Peptides

Peptide	Source	Start position	Amino acid sequence	HLA restriction
$MRP3_{503}$	MRP3	503	LYAWEPSFL	HLA-A24
$MRP3_{692}$	MRP3	692	AYVPQQAWI	HLA-A24
$MRP3_{765}$	MRP3	765	VYSDADIFL	HLA-A24
HIV env_{584}	HIV envelope	584	RYLRDQQLL	HLA-A24
CMV $pp65_{328}$	CMV pp65	328	QYDPVAALF	HLA-A24
AFP_{403}	AFP	403	KYIQESQAL	HLA-A24

was <15% of the maximum release for all experiments. For the assay using hepatoma cell lines, the cytotoxic activity was considered positive when it was higher than that of CTL against K562 which shows non-specific lysis. The assay was performed at least three times for each peptide.

2.7. ELISPOT assay

ELISPOT assays were performed as previously described with the following modifications [9,10]. Peptides $MRP3_{503}$, $MRP3_{692}$, and $MRP3_{765}$ were used for the detection of MRP3-specific T cells. Negative controls consisted of a HIV envelope-derived peptide ($HIVenv_{584}$) [24]. Positive controls consisted of 10 ng/ml phorbol 12-myristate 13-acetate (PMA, Sigma) or a CMV pp65-derived peptide ($CMVpp65_{328}$) [25]. The colored spots were counted with a KS ELISpot Reader (Zeiss, Tokyo, Japan). The number of specific spots was determined by subtracting the number of spots in the absence of antigen from the number of spots in its presence. Responses for peptides $MRP3_{503}$, $MRP3_{692}$, and $MRP3_{765}$ in HCC patients were considered positive if more than the mean + 3SD specific spots in healthy normal donors were detected and if the number of spots in the presence of antigen was at least twofold greater than the number of spots in its absence. Responses for peptides $HIVenv_{584}$ and $CMVpp65_{328}$ were considered positive if more than 10 specific spots were detected and if the number of spots in the presence of antigen was at least twofold greater than the number of spots in the absence of antigen.

2.8. Tetramer staining and flow cytometry

Peptide $MRP3_{765}$ specific tetramer was purchased from Medical Biological Laboratories Co., Ltd (Nagoya, Japan). Tetramer staining was performed according to a previously reported method with several modifications [10]. In brief, PBMCs were stained with CD8-PerCP (BD PharMingen, San Diego, CA, USA) and tetramer-PE (10 μl) for 30 min at room temperature. Cells were washed, fixed with 0.5% paraformaldehyde/PBS, and analyzed on a FACSCalibur™ flow cytometer. Data analysis was undertaken with CELLQuest™ software (Becton–Dickinson, San Jose, CA, USA).

2.9. Statistical analysis

Data are expressed as means ± SD. The χ^2 test with Yates' correction, Fisher's exact probability test, and the unpaired t-test were used for statistical analyses where appropriate. Linear regression lines for the relationship between expression of MRP3 mRNA and MRP3-specific immune responses were calculated using Pearson's correlation coefficient. A level of $P < 0.05$ was considered significant.

3. Results

3.1. Patient profile

The clinical profiles of the patients are shown in Table 1. In 52 patients, HCC was histologically classified as well-, moderately, and poorly differentiated HCC in 17, 31, and 4, respectively. In the other patients, HCC was diagnosed based on typical CT findings and AFP elevation. On tumor classification based on the size and number, the tumor was large (>2 cm) in 79, small (≤2 cm) in 24, multiple in 73, and solitary in 30. Vascular invasion was noted in 30 patients. On tumor classification using the TNM staging of the Union Internationale Contre Le Cancer (UICC) classification system (6th version), 24, 51, 16, 1, 3, and 8 patients were staged I, II, IIIA, IIIB, IIIC, and IV, respectively.

3.2. Expression of MRP3 in hepatoma cell lines and HCC tissues

To investigate the MRP3 expression level in HCC, we measured MRP3 mRNA in 8 hepatoma cell lines by real-time PCR. The expression ratio of MRP3 to β-actin, measured as an internal control, is shown in Fig. 1A. All hepatoma cell lines except HLF expressed MRP3, but the expression level varied among the cell lines. HepG2, Hep3B and Huh7 showed high expression levels, but Alex, HLE, SKHep1 and Huh6 showed low expression levels.

The MRP3 expression level in HCC tissues was compared with non-cancerous tissues in specimens obtained from 20 HCC patients by US-guided needle tumor biopsy or surgical resection. The MRP3 expression level was significantly higher in HCC tissue than in the non-cancerous tissue ($P < 0.05$) (Fig. 1B). In the analysis of the individual MRP3 expression levels, 11 of 20 (55%) HCC tissues showed higher expression level than that of Huh 7 whose average of expression level is 1.0 (Fig. 1C).

3.3. Cytotoxic activity of MRP3 peptide-specific CTL against hepatoma cell lines

Whether the MRP3-derived peptides used were capable of inducing peptide-specific CTL from PBMCs was investigated in at least 10 HCC patients. The CTLs specific for $MRP3_{503}$, $MRP3_{692}$, and $MRP3_{765}$ were induced in 3, 3 and 2 patients, respectively. As shown in Fig. 2A, all CTL induced with $MRP3_{503}$, $MRP3_{692}$, and $MRP3_{765}$ showed high-level cytotoxicity against C1RA24 cells pulsed with the corresponding peptides.

These CTLs exhibited cytotoxicity against hepatoma cell lines with the HLA-A24 molecule and high expression of MRP3, HepG2 and HLE, but not against MRP3-hypoexpressing Huh6 and MRP3-overexpressing Huh7 without HLA-A24 molecule (Fig. 2B).

3.4. T Cell responses to MRP3-derived peptides assessed by IFN-γ ELISPOT analysis

To determine a significant number of T cells that specifically reacted with $MRP3_{503}$, $MRP3_{692}$ and $MRP3_{765}$

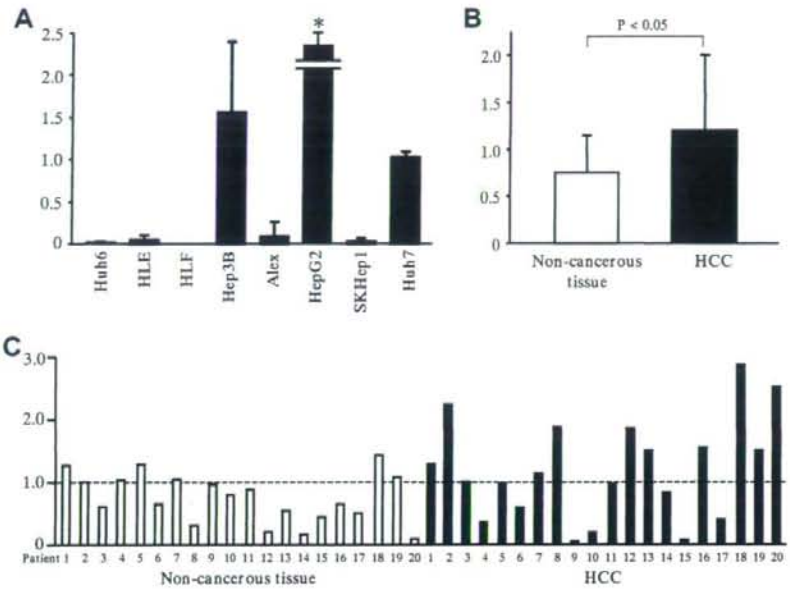

Fig. 1. Expression levels of MRP3 mRNA. (A) Expression of MRP3 mRNA was measured by real-time PCR in hepatoma cell lines. (B) Comparison of MRP3 mRNA expression levels between non-tumor (white bar) and tumor (solid bar) tissues. The data are expressed as means + SD. The unpaired *t*-test was used for a statistical analysis. (C) Comparison of MRP3 mRNA expression levels between non-tumor (white bar) and tumor (solid bar) tissues in individual HCC patients. * denotes 6.15 + 4.21.

peptides in HCC patients, ELISPOT assays were performed using PBMCs from 11 healthy donors. The number of specific spots was 0.2 ± 0.5, 1.5 ± 2.1, 0.9 ± 1.0, 1.3 ± 2.0, and 13.3 ± 15.7 cells/3×10^5 PBMCs, respectively (Fig. 3). Similarly, cells that specifically reacted with the peptides were counted in HCC patient-derived PBMCs. Regarding a number of T cells that specifically reacted with the peptide of larger than the mean + 3SD of that in healthy donor-derived PBMCs as a significant response, 20.0, 14.1, and 21.4% of the patients showed significant responses to $MRP3_{503}$, $MRP3_{692}$, and $MRP3_{765}$, respectively (Fig. 4A). A significant response specific for $CMVpp65_{328}$ was detected in 51.0% and 36.4% of the HCC patients and healthy donors, respectively, showing no significant difference between the 2 groups. On the other hand, no significant response for $HIVenv_{584}$ was observed in both groups.

On similar analysis of TIL, 75.0, 75.0, and 37.5% of the patients showed significant responses to $MRP3_{503}$, $MRP3_{692}$, and $MRP3_{765}$, respectively, revealing that the frequencies were higher than those in PBMCs (Fig. 4B).

3.5. Detection of $MRP3_{765}$ tetramer$^+$ and CD8$^+$ T lymphocytes in PBMCs

The frequency of MRP3-specific T cells was also investigated using $MRP3_{765}$ tetramer in 20 HCC patients. To confirm the specificity of $MRP3_{765}$ tetramer, we tried to detect the tetramer$^+$ cells in a CTL line induced by stimulation with $MRP3_{765}$ peptide. The frequency of $MRP3_{765}$ tetramer$^+$ cells in CD8$^+$ cells was increased from 0.03% before to 9.15% after stimulation (Fig. 5A). When PBMC was stimulated with irrelevant peptide (AFP_{403}), the frequency of $MRP3_{765}$ tetramer$^+$ cells was only 0.08%.

To count the frequency of tetramer$^+$ cells in peripheral blood, we used freshly isolated non-stimulated PBMCs for the assay. The tetramer$^+$ and CD8$^+$ T cells accounted for 0.00–0.23% in PBMCs of HCC patients (Fig. 5B). Next, the results were compared with those of ELISPOT assay. In patients 1 to 7, both $MRP3_{765}$ tetramer$^+$ and IFN-γ producing cells responding to the peptide in ELISPOT assay were detected. In contrast, in patients 8 to 13, the frequency of tetramer$^+$ cells was high, but no significant increase in the $MRP3_{765}$ peptide-specific T cell count was detected by the ELISPOT assay.

3.6. MRP3-specific T cell responses and clinical features of HCC patients

To clarify the clinical characteristics of MRP3-specific T cell responses in HCC patients, the clinical background was compared between patients who showed positive responses to MRP3-derived peptides on ELISPOT assay and those who did not. No significant differences were noted between the 2 groups (Table 3).

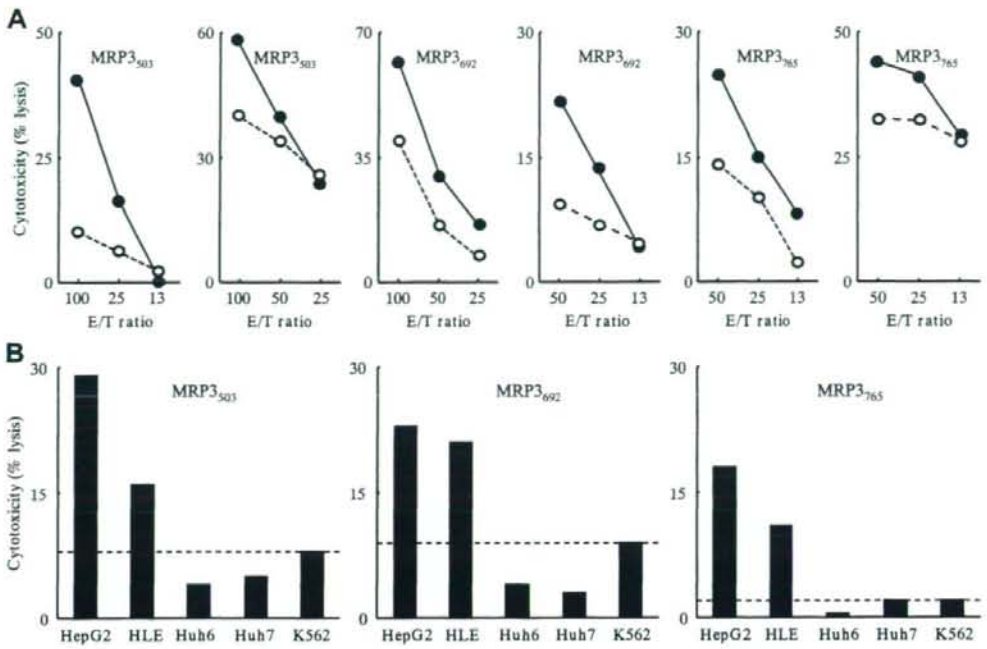

Fig. 2. Cytotoxicity of MRP3-specific T-cell lines derived with peptide in patients with HCC. (A) The cytotoxicity of T-cell lines was determined by a standard 6-h cytotoxicity assay at various effector to target (E/T) ratios against C1R-A*2402 cells pulsed with or without one of the MRP3-derived peptides listed in Table 2. The open circle shows the cytotoxicity against C1R-A*2402 cells pulsed without a peptide. The closed circle shows the cytotoxicity against C1R-A*2402 cells pulsed with a peptide. (B) Cytotoxicity of MRP3-specific T-cell lines derived with peptide was also measured against hepatoma cell lines. The cytotoxicity was considered positive when it was higher than that against K562 which shows non-specific lysis. HepG2 expresses MRP3 and has HLA-A*2402. Huh 6 and HLE show a low expression of MRP3 and have HLA-A*2402. Huh 7 shows MRP3 expression, but does not have HLA-A*2402. Cytotoxicity was determined by a standard 6-h cytotoxic assay (E/T ratio of 50:1).

In 20 HCC patients in whom the MRP3 expression level in HCC tissue could be measured, the relationship between the expression level and frequency of MRP3-specific T cells was investigated. A significant negative correlation was present between the MRP3 expression level in HCC tissue and MRP3-specific T cell frequency ($r = -0.54$, $P < 0.05$) (Fig. 6A). When the relationship between the MRP3 expression level in HCC tissue and CMVpp65-specific T-cell frequency was similarly analyzed, no significant correlation was present. Furthermore, when the patients were divided into groups with high and low HCC tissue MRP3 expression levels, setting the border to the mean MRP3 expression level in the normal liver tissues, 0.743, the peripheral blood MRP3-specific T cell frequency was significantly higher in the low- than in the high-level group ($p < 0.05$) (Fig. 6B). The CMVpp65-specific T cell frequency was not significantly different between the 2 groups.

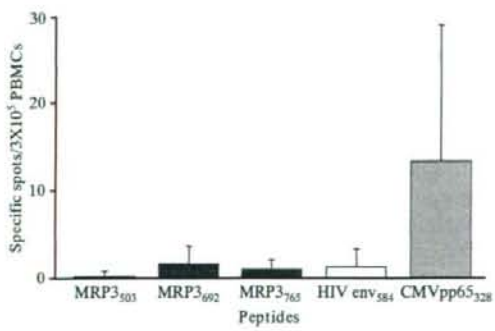

Fig. 3. Direct ex-vivo analysis (IFN-γ ELISPOT assay) of peripheral blood T cell responses to MRP3-derived peptides (peptides $MRP3_{503}$, $MRP3_{692}$, and $MRP3_{765}$: solid bars) or control peptides (peptides $HIVenv_{584}$ and $CMVpp65_{328}$: open and grey bars, respectively) in healthy normal donors. The data are expressed as means + SD.

3.7. Enhancement of MRP3-specific T cell responses after anti-cancer treatment

Several studies including our report have clarified that HCC treatment enhanced HCC-specific immune responses [9,26,27]. We investigated whether MRP3-specific T cell responses observed in HCC patients were enhanced by HCC treatment. In 12 patients who underwent TAE or radiofrequency ablation (RFA) or both

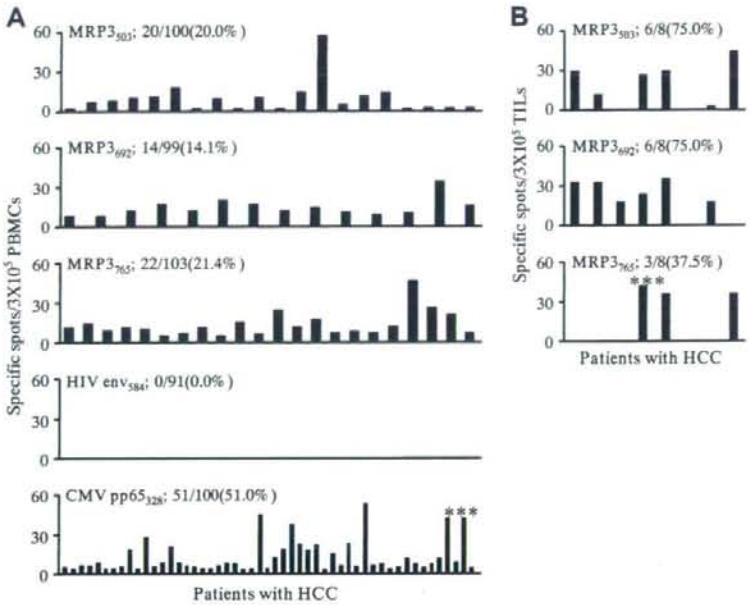

Fig. 4. Direct ex-vivo analysis (IFN-γ ELISPOT assay) of PBMCs (A) and TILs (B) response to MRP3-derived peptides (peptides $MRP3_{503}$, $MRP3_{692}$, and $MRP3_{765}$) or control peptides (peptides $HIVenv_{584}$ and $CMVpp65_{328}$) in HCC patients. Only significant IFN-γ responses are included. Responses to peptides $MRP3_{503}$, $MRP3_{692}$, and $MRP3_{765}$ were considered positive if more than the mean + 3SD specific spots in healthy normal donors were detected and if the number of spots in the presence of antigen was at least twofold greater than that in its absence. Responses to peptides $HIVenv_{584}$ and $CMVpp65_{328}$ were considered positive if more than 10 specific spots were detected and if the number of spots in the presence of antigen was at least twofold greater than that in its absence. The peptide sequences are described in Table 2. * denotes 770 specific spots. ** denotes 210 specific spots. * denotes 72 specific spots.**

without MRP3-specific T-cell responses before treatment, changes in the MRP3-specific T cell frequency were investigated by measuring the frequency by ELISPOT assay before and after treatment. The $MRP3_{503}$, $MRP3_{692}$, or $MRP3_{765}$ peptide-specific T cell frequency was increased after treatment in 8 of the 12 patients (Table 4). In contrast, the immune response to $HIVenv_{584}$ peptide was not enhanced in any patient, and that to $CMVpp65_{328}$ peptide was enhanced in one patient.

4. Discussion

The expression of MRP3 has been reported in several normal tissues and cancer cells [14,15,28,29]. Although MRP3 expression in HCC tissue was confirmed by immunohistochemical staining [16], the expression level varied among patients, and a conclusion has not been reached as to whether the expression is increased compared to that in normal liver tissue [16,17]. In this study, MRP3 expression in HCC tissue was detected in all 20 HCC patients, and the expression level was significantly higher than that in non-cancerous tissue.

The presence of MRP3-recognizing CTL has been reported in lung, colon, bladder, and renal cancer patients [13,30]. However, to our knowledge, there is no report showing the presence of MRP3-specific CTL in HCC patients. In this study, we showed that MRP3-specific CTL could be induced by stimulating PBMCs with MRP3-derived peptides, and the induced CTL showed cytotoxicity against hepatoma cell lines overexpressing MRP3. Based on these findings, we confirmed that MRP3-specific CTLs exist in HCC patients and MRP3 serves as an immunogenic antigen in HCC.

The frequency of peripheral blood CTL specific to each MRP3 epitope was similar to the reported frequencies of CTL against other tumor antigen epitopes [9,10,31–33]. The CTLs were induced even in an early stage of HCC and regardless of HCV infection. In TILs, MRP3-specific CTL were more frequently detected, compared to that in peripheral blood, suggesting that MRP3-specific CTL are not only present in peripheral blood but also infiltrate into the tumor.

The presence and frequency of MRP3-specific CTL were also confirmed using $MRP3_{765}$ tetramer. However, MRP3-specific CTL could not be detected by ELISPOT assay in 6 patients despite a high frequency being

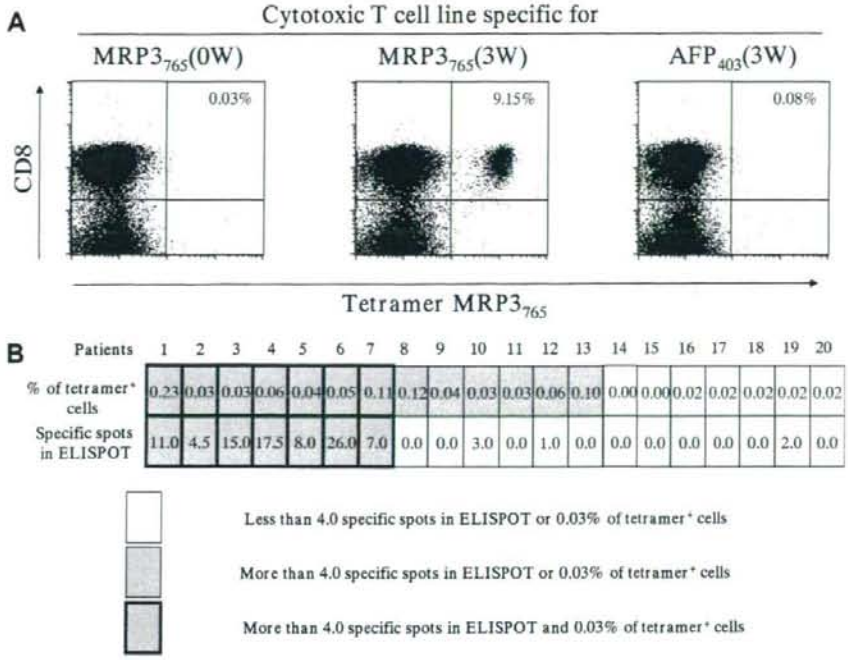

Fig. 5. Detection of MRP3-specific, HLA-A*2402-tetramer$^+$ and CD8$^+$ T lymphocytes in the peripheral blood. (A) Specificity of the $MRP3_{765}$ tetramer was confirmed by staining peptide-specific and non-specific in vitro-expanded T-cell lines. (B) Analysis of the association between the frequency of tetramer$^+$ cells and IFN-γ-producing cells detected on ELISPOT assay was performed in 20 patients.

detected by the tetramer. These findings were similar to those of hTERT-specific CTL in our previous study [10], suggesting the presence of MRP3-specific non-functional T cells in HCC patients.

In the analysis of association between the HCC tissue MRP3 expression level and MRP3-specific T-cell frequency in peripheral blood, a negative correlation was detected, suggesting that MRP3-specific immune responses exert an immune pressure on MRP3-expressing HCC cells. Recent studies have shown the involvement of MRP3 in the resistance to anti-tumor drugs and poor prognosis in several cancer patients [14,15,28,29,34,35]. Taken together with these reports, our results suggest the possibility that MRP3-targeting immunotherapy not only simply eliminates cancers but also improves drug resistance and the prognosis by inhibiting MRP3 expression in cancer cells.

Further to evaluate the usefulness of MRP3 in HCC immunotherapy, we also investigated the association between HCC treatment and the MRP3-specific CTL frequency. As we and other groups previously reported [9,26,27], the MRP3-specific CTL frequency was increased after treatment in 8 of the 12 patients in whom no immune response to MRP3 was detected before treatment, whereas the HIV env_{584}- and $CMVpp65_{328}$-specific CTL frequencies were not increased, excluding one patient, suggesting that this phenomenon represents the enhancement of MRP3-specific immune responses. These findings also confirmed that MRP3 is an antigen expressed in HCC tis-

Table 3
Univariate analysis of the effect of variables on the T cell response against MRP3

	Patients with positive T cell response	Patients without positive T cell response	*p*-value[a]
No. of patients	38	65	
Age (years)[b]	61.4 ± 10.0	64.3 ± 9.7	NS
Sex (M/F)	30/8	49/16	NS
AFP level (≤20/>20)	17/21	21/44	NS
Diff. degree of HCC (well/moderate or poor/ND)[c]	5/14/19	12/21/32	NS
Tumor multiplicity (multiple/solitary)	30/8	43/22	NS
Vascular invasion (+/−)	12/26	18/47	NS
TNM factor			
(T1/T2–4)	6/32	18/47	NS
(N0/N1)	36/2	64/1	NS
(M0/M1)	36/2	57/8	NS
TNM stage (I/II–IV)	6/32	18/47	NS
Histology of non-tumor liver (LC/chronic hepatitis)	30/8	55/10	NS
Liver function (Child A/B/C)	23/14/1	38/25/2	NS
Etiology (HCV/HBV/others)	26/7/5	49/12/4	NS

[a] NS, not significant.
[b] Data are expressed as means ± SD.
[c] ND, not determined.

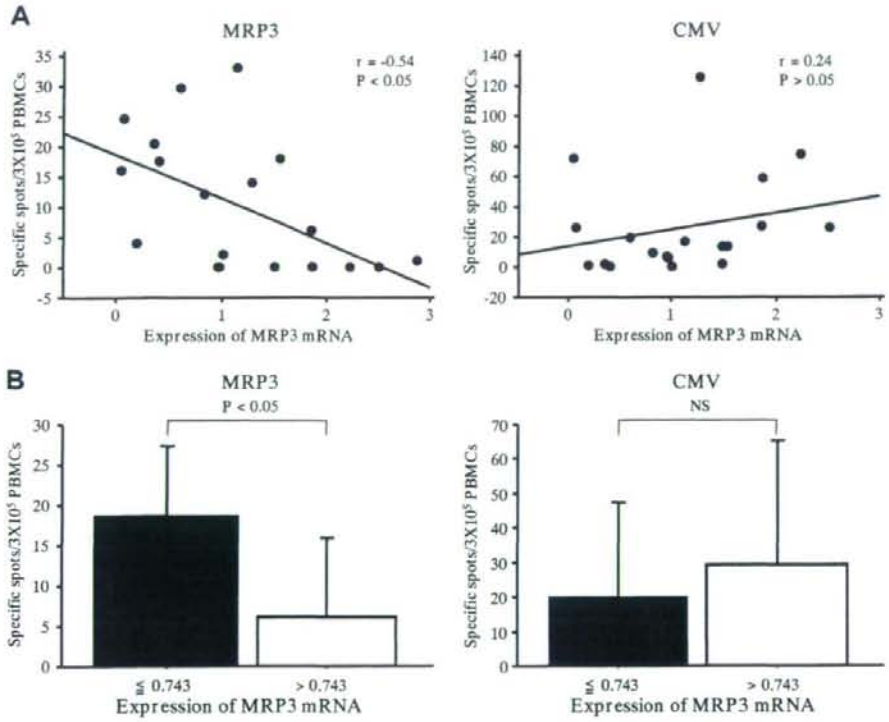

Fig. 6. Analysis of the association between the frequencies of MRP3- specific T cells detected on ELSPOT assay and the expression levels of MRP3 mRNA in HCC tissues. The frequency of MRP3-specific T cells was calculated by the sum of specific spots against $MRP3_{503}$, $MRP3_{692}$, and $MRP3_{765}$ peptides. (A) Linear regression lines for the relationship between the expression of MRP3 mRNA and the frequency of MRP3- or CMVpp65-specific T cells were calculated using Pearson's correlation coefficient. (B) Analysis of the frequency of MRP3- or CMVpp65-specific T cells in patients with low and high expression levels of MRP3 mRNA in HCC tissues.

sue, and has strong immunogenicity that readily induces CTL in vivo.

In conclusion, our study demonstrates that MRP3 is a potential candidate for tumor antigen with strong immunogenicity in HCC immunotherapy.

Acknowledgements

The authors thank Maki Kawamura, Kazumi Fushimi, Nami Nishiyama and Mikiko Nakamura for technical assistance.

Table 4
T cell response to MRP3-derived peptides by ELISPOT assay before and after treatment

	Treatment[a]	Before treatment					After treatment				
		$MRP3_{503}$	$MRP3_{692}$	$MRP3_{765}$	$HIVenv_{584}$	$CMVpp65_{328}$	$MRP3_{503}$	$MRP3_{692}$	$MRP3_{765}$	$HIVenv_{584}$	$CMVpp65_{328}$
Patient 1	TAE + RF	1	0	0	0	9	**5**	5	3	2	6
Patient 2	TAE + RF	0	0	0	0	0	**2**	2	0	0	2
Patient 3	TAE + RF	0	2	0	4	5	**8**	1	**6**	2	**13**
Patient 4	TAE + RF	0	0	0	0	**16**	0	0	0	0	**46**
Patient 5	TAE + RF	0	4	0	1	3	**5**	0	**37**	0	ND[b]
Patient 6	TAE + RF	0	0	0	0	**61**	0	0	4	1	**59**
Patient 7	TAE	0	0	0	0	**92**	0	0	**6**	0	**129**
Patient 8	TAE	0	1	0	1	9	0	1	0	0	0
Patient 9	RF	0	0	0	0	**74**	**6**	7	2.5	2.5	**65**
Patient 10	RF	0	0	0	0.5	0	**3**	0	1	0.5	9.5
Patient 11	RF	1.5	0	1	1	9.5	0	3	**9.5**	1	5.5
Patient 12	RF	0	0	0	0	**13**	0	0	0	0	6

Bold and underlined letters indicate a significant increase as described in materials and methods.

[a] TAE, transcatheter arterial embolization; RF, radiofrequency ablation.

[b] ND: not determined.

References

[1] Llovet JM, Burroughs A, Bruix J. Hepatocellular carcinoma. Lancet 2003;362:1907–1917.

[2] Lin SM, Lin CJ, Lin CC, Hsu CW, Chen YC. Radiofrequency ablation improves prognosis compared with ethanol injection for hepatocellular carcinoma < or =4 cm. Gastroenterology 2004;127:1714–1723.

[3] Ercolani G, Grazi GL, Ravaioli M, Del Gaudio M, Gardini A, Cescon M, et al. Liver resection for hepatocellular carcinoma on cirrhosis: univariate and multivariate analysis of risk factors for intrahepatic recurrence. Ann Surg 2003;237:536–543.

[4] Omata M, Tateishi R, Yoshida H, Shiina S. Treatment of hepatocellular carcinoma by percutaneous tumor ablation methods: ethanol injection therapy and radiofrequency ablation. Gastroenterology 2004;127:S159–S166.

[5] Butterfield LH, Ribas A, Meng WS, Dissette VB, Amarnani S, Vu HT, et al. T-cell responses to HLA-A*0201 immunodominant peptides derived from alpha-fetoprotein in patients with hepatocellular cancer. Clin Cancer Res 2003;9:5902–5908.

[6] Shang XY, Chen HS, Zhang HG, Pang XW, Qiao H, Peng JR, et al. The spontaneous CD8+ T-cell response to HLA-A2-restricted NY-ESO-1b peptide in hepatocellular carcinoma patients. Clin Cancer Res 2004;10:6946–6955.

[7] Zerbini A, Pilli M, Soliani P, Ziegler S, Pelosi G, Orlandini A, et al. Ex vivo characterization of tumor-derived melanoma antigen encoding gene-specific CD8+cells in patients with hepatocellular carcinoma. J Hepatol 2004;40:102–109.

[8] Komori H, Nakatsura T, Senju S, Yoshitake Y, Motomura Y, Ikuta Y, et al. Identification of HLA-A2- or HLA-A24-restricted CTL epitopes possibly useful for glypican-3-specific immunotherapy of hepatocellular carcinoma. Clin Cancer Res 2006;12:2689–2697.

[9] Mizukoshi E, Nakamoto Y, Tsuji H, Yamashita T, Kaneko S. Identification of alpha-fetoprotein-derived peptides recognized by cytotoxic T lymphocytes in HLA-A24+ patients with hepatocellular carcinoma. Int J Cancer 2006;118:1194–1204.

[10] Mizukoshi E, Nakamoto Y, Marukawa Y, Arai K, Yamashita T, Tsuji H, et al. Cytotoxic T cell responses to human telomerase reverse transcriptase in patients with hepatocellular carcinoma. Hepatology 2006;43:1284–1294.

[11] Borst P, Elferink RO. Mammalian ABC transporters in health and disease. Annu Rev Biochem 2002;71:537–592.

[12] Kiuchi Y, Suzuki H, Hirohashi T, Tyson CA, Sugiyama Y. cDNA cloning and inducible expression of human multidrug resistance associated protein 3 (MRP3). FEBS Lett 1998;433:149–152.

[13] Yamada A, Kawano K, Koga M, Matsumoto T, Itoh K. Multidrug resistance-associated protein 3 is a tumor rejection antigen recognized by HLA-A2402-restricted cytotoxic T lymphocytes. Cancer Res 2001;61:6459–6466.

[14] Tada Y, Wada M, Migita T, Nagayama J, Hinoshita E, Mochida Y, et al. Increased expression of multidrug resistance-associated proteins in bladder cancer during clinical course and drug resistance to doxorubicin. Int J Cancer 2002;98:630–635.

[15] Young LC, Campling BG, Cole SP, Deeley RG, Gerlach JH. Multidrug resistance proteins MRP3, MRP1, and MRP2 in lung cancer: correlation of protein levels with drug response and messenger RNA levels. Clin Cancer Res 2001;7:1798–1804.

[16] Nies AT, Konig J, Pfannschmidt M, Klar E, Hofmann WJ, Keppler D. Expression of the multidrug resistance proteins MRP2 and MRP3 in human hepatocellular carcinoma. Int J Cancer 2001;94:492–499.

[17] Zollner G, Wagner M, Fickert P, Silbert D, Fuchsbichler A, Zatloukal K, et al. Hepatobiliary transporter expression in human hepatocellular carcinoma. Liver Int 2005;25:367–379.

[18] Araki T, Itai Y, Furui S, Tasaka A. Dynamic CT densitometry of hepatic tumors. AJR Am J Roentgenol 1980;135:1037–1043.

[19] Liver cancer study group of Japan. General rules for the clinical and pathological study of primary liver cancer. Second English Edition. Kanehara & Co., Ltd., Tokyo. 2003.

[20] Desmet VJ, Gerber M, Hoofnagle JH, Manns M, Scheuer PJ. Classification of chronic hepatitis: diagnosis, grading and staging. Hepatology 1994;19:1513–1520.

[21] Oiso M, Eura M, Katsura F, Takiguchi M, Sobao Y, Masuyama K, et al. A newly identified MAGE-3-derived epitope recognized by HLA-A24-restricted cytotoxic T lymphocytes. Int J Cancer 1999;81:387–394.

[22] Honda M, Yamashita T, Ueda T, Takatori H, Nishino R, Kaneko S. Different signaling pathways in the livers of patients with chronic hepatitis B or chronic hepatitis C. Hepatology 2006;44:1122–1138.

[23] Mizukoshi E, Nascimbeni M, Blaustein JB, Mihalik K, Rice CM, Liang TJ, et al. Molecular and immunological significance of chimpanzee major histocompatibility complex haplotypes for hepatitis C virus immune response and vaccination studies. J Virol 2002;76:6093–6103.

[24] Ikeda-Moore Y, Tomiyama H, Miwa K, Oka S, Iwamoto A, Kaneko Y, et al. Identification and characterization of multiple HLA-A24-restricted HIV-1 CTL epitopes: strong epitopes are derived from V regions of HIV-1. J Immunol 1997;159:6242–6252.

[25] Kuzushima K, Hayashi N, Kimura H, Tsurumi T. Efficient identification of HLA-A*2402-restricted cytomegalovirus-specific CD8(+) T-cell epitopes by a computer algorithm and an enzyme-linked immunospot assay. Blood 2001;98:1872–1881.

[26] Zerbini A, Pilli M, Penna A, Pelosi G, Schianchi C, Molinari A, et al. Radiofrequency thermal ablation of hepatocellular carcinoma liver nodules can activate and enhance tumor-specific T-cell responses. Cancer Res 2006;66:1139–1146.

[27] Ayaru L, Pereira SP, Alisa A, Pathan AA, Williams R, Davidson B, et al. Unmasking of alpha-fetoprotein-specific CD4(+) T cell responses in hepatocellular carcinoma patients undergoing embolization. J Immunol 2007;178:1914–1922.

[28] Konig J, Hartel M, Nies AT, Martignoni ME, Guo J, Buchler MW, et al. Expression and localization of human multidrug resistance protein (ABCC) family members in pancreatic carcinoma. Int J Cancer 2005;115:359–367.

[29] Steinbach D, Wittig S, Cario G, Viehmann S, Mueller A, Gruhn B, et al. The multidrug resistance-associated protein 3 (MRP3) is associated with a poor outcome in childhood ALL and may account for the worse prognosis in male patients and T-cell immunophenotype. Blood 2003;102:4493–4498.

[30] Komohara Y, Harada M, Arima Y, Suekane S, Noguchi M, Yamada A, et al. Anti-cancer vaccine candidates in specific immunotherapy for bladder carcinoma. Int J Oncol 2006;29:1555–1560.

[31] Nagorsen D, Keilholz U, Rivoltini L, Schmittel A, Letsch A, Asemissen AM, et al. Natural T-cell response against MHC class I epitopes of epithelial cell adhesion molecule, her-2/neu, and carcinoembryonic antigen in patients with colorectal cancer. Cancer Res 2000;60:4850–4854.

[32] Griffioen M, Borghi M, Schrier PI, Osanto S. Detection and quantification of CD8(+) T cells specific for HLA-A*0201-binding melanoma and viral peptides by the IFN-gamma-ELISPOT assay. Int J Cancer 2001;93:549–555.

[33] Rentzsch C, Kayser S, Stumm S, Watermann I, Walter S, Stevanovic S, et al. Evaluation of pre-existent immunity in patients with primary breast cancer: molecular and cellular assays to quantify antigen-specific T lymphocytes in peripheral blood mononuclear cells. Clin Cancer Res 2003;9:4376–4386.

[34] Oguri T, Isobe T, Fujitaka K, Ishikawa N, Kohno N. Association between expression of the MRP3 gene and exposure to platinum drugs in lung cancer. Int J Cancer 2001;93:584–589.

[35] Steinbach D, Lengemann J, Voigt A, Hermann J, Zintl F, Sauerbrey A. Response to chemotherapy and expression of the genes encoding the multidrug resistance-associated proteins MRP2, MRP3, MRP4, MRP5, and SMRP in childhood acute myeloid leukemia. Clin Cancer Res 2003;9:1083–1086.

ELSEVIER

Journal of Hepatology 49 (2008) 207–216

Journal of Hepatology

www.elsevier.com/locate/jhep

Identification of novel candidate tumour marker genes for intrahepatic cholangiocarcinoma☆

Ryuhei Nishino[1], Masao Honda[1], Taro Yamashita[1], Hajime Takatori[1], Hiroshi Minato[2], Yoh Zen[2], Motoko Sasaki[3], Hiroyuki Takamura[4], Katsuhisa Horimoto[5], Tetsuo Ohta[4], Yasuni Nakanuma[3], Shuichi Kaneko[1,*]

[1]*Department of Gastroenterology, Kanazawa University Graduate School of Medical Science, Kanazawa University, 13-1 Takara-Machi, Kanazawa 920-8641, Japan*
[2]*Pathology Section, Kanazawa University Hospital, Kanazawa University, 13-1 Takara-Machi, Kanazawa 920-8641, Japan*
[3]*Department of Human Pathology, Kanazawa University Graduate School of Medical Science, Kanazawa University, 13-1 Takara-Machi, Kanazawa 920-8641, Japan*
[4]*Department of Gastroenterologic Surgery, Kanazawa University Graduate School of Medical Science, Kanazawa University, 13-1 Takara-Machi, Kanazawa 920-8641, Japan*
[5]*Biological Network Team, Computational Biology Research Centre, National Institute of Advanced Industrial Science and Technology, Japan*

See Editorial, pages 160–162

***Background/Aims*: Specific markers are required for early detection and diagnosis of intrahepatic cholangiocarcinoma (ICC); however, the tumour markers currently in use are not specific for ICC.**

***Methods*: We compared an ICC cDNA library with that of hepatocellular carcinoma (HCC) by serial analysis of gene expression (SAGE). The expression patterns in each were confirmed by quantitative real-time reverse transcriptase-polymerase chain reaction (RT-PCR), immunoblotting and immunohistochemical analysis of 74 samples including 16 ICC samples.**

***Results*: A comparison of the two libraries revealed distinct gene expression patterns for each type of liver cancer. In addition to the known tumour markers, we detected nine novel genes associated with ICC. By comparing the mean transcript abundance in the ICC library with those in other libraries, including gastric, colon, prostate and breast cancer, together with our RT-PCR results, we identified three genes as specific markers of ICC: biglycan, insulin-like growth factor-binding protein 5 and claudin-4. Immunoblotting and immunohistochemical analyses showed that claudin-4 was highly expressed in ICC. Moreover, discrimination analysis revealed that a combination of these genes could be used to distinguish ICC from HCC or metastatic adenocarcinoma.**

***Conclusions*: We identified novel marker genes of ICC that are potentially useful for the diagnosis of liver cancer.**

***Keywords*: Differential diagnosis; Hepatocellular carcinoma; Intrahepatic cholangiocarcinoma; SAGE**

Received 5 October 2007; received in revised form 10 March 2008; accepted 24 March 2008; available online 5 May 2008
Associate Editor: J.M. Llovet

☆ The authors declare that they do not have anything to disclose regarding funding from industries or conflict of interest with respect to this manuscript.

* Corresponding author. Tel.: +81 76 265 2231; fax: +81 76 234 4250.
E-mail address: skaneko@m-kanazawa.jp (S. Kaneko).

Abbreviations: ICC, intrahepatic cholangiocarcinoma; HCC, hepatocellular carcinoma; AFP, alpha-foetoprotein; KRT, keratin; CEA, carcinoembryonic antigen; CA19-9, carbohydrate antigen 19-9; SAGE, serial analysis of gene expression; HBV, hepatitis B virus; HCV, hepatitis C virus; NL, normal liver; CLD, chronic liver disease; RT-PCR, reverse transcriptase-polymerase chain reaction; polyA-RNA, polyadenylated RNA; mRNA, messenger RNA; GAPDH, glyceraldehyde-3-phosphate dehydrogenase; CITED4, Cbp/p300-interacting transactivator with Glu/Asp-rich carboxy-terminal domain 4; GSTP1, glutathione-*S*-transferase pi; BGN, biglycan; IGFBP5, insulin-like growth factor-binding protein 5; CLDN4, claudin-4; PFKP, platelet type phosphofructokinase; TM4SF1, transmembrane 4 L six family member 1; CAPN1, calpain 1 (μ/l) large subunit; CLDN10, claudin-10; S100A6, S100 calcium-binding protein A6; Wnt, wingless-type MMTV integration site; TGF-beta, transforming growth factor-beta.

0168-8278/$34.00
doi:10.1016/j.jhep.2008.03.025

1. Introduction

Intrahepatic cholangiocarcinoma (ICC), which arises from bile duct cells in the liver, currently accounts for approximately 15% of primary liver cancer [1]. Though it is less familiar than hepatocellular carcinoma (HCC), the incidence of ICC is increasing, especially in the United States, the United Kingdom and Australia [2–5].

The differential diagnosis of liver cancer depends on a combination of serological, radiological and histological examinations; however, the process can be difficult, especially in advanced stages. In addition, liver cancer may include metastasis from other organs, making the diagnosis even more difficult. Nevertheless, a correct diagnosis is essential to select the proper therapy and to determine a patient's prognosis.

Tumour markers are routinely used in the differential diagnosis of liver cancer. For example, alpha-foetoprotein (AFP) is a sensitive and specific marker of HCC [6]; keratin (KRT) 7 and KRT19 are amongst the markers of ICC. KRT7 and KRT19, which are expressed in the bile duct epithelium and ICC [7–10], can be used to distinguish HCC from ICC immunohistochemically. These are not specific to ICC, however, and are expressed in other cancers such as non-small-cell lung carcinoma [11]. Other proteins such as carcinoembryonic antigen (CEA) and carbohydrate antigen 19-9 (CA19-9) have been used as serum markers for ICC [12,13], but these are also not specific to ICC because they are overexpressed in other malignant tumours. Thus, identifying ICC-specific markers will be valuable for differentially diagnosing liver cancer to characterise ICC at the molecular level and to develop improved therapies for patients with ICC. Recently, Lodi et al. cited claudin-4 (CLDN4) expression as a possible marker in differentiating biliary tract cancers from HCC [14]. However, the gene's ability to distinguish metastatic liver cancer has not been evaluated.

In recent years, serial analysis of gene expression (SAGE) [15] and DNA microarrays have been used to comprehensively analyse gene expression, including comparisons of the expression patterns in normal liver [16] and HCC [17–19]. We used SAGE to construct cDNA libraries of ICC and HCC and performed comprehensive analyses of the expression patterns in these tumours to identify novel markers of ICC.

2. Materials and methods

2.1. Tissue samples

For SAGE analysis, we prepared one ICC sample and three HCC samples (Table 1). The ICC sample was obtained by the surgical resection of a solitary cancerous lesion in the liver, which was diagnosed histopathologically as a moderately differentiated cholangiocellular carcinoma (Fig. 1A). The HCC samples were obtained from three surgically resected cancerous lesions, all of which were diagnosed histopathologically as well-differentiated HCCs (Fig. 1B). The clinical characteristics of the patients are provided in Table 1.

In total, 74 samples (i.e., 16 ICC, seven normal liver (NL), 20 chronic liver disease (CLD), 26 HCC (Tables 1 and 2) and five extrahepatic adenocarcinoma) were used for quantitative real-time reverse transcriptase-polymerase chain reaction detection (RT-PCR) and discrimination analyses. The NL samples were obtained by the surgical resection of colon tumours from patients with metastatic liver cancer, whereas the CLD samples were non-cancerous liver samples obtained from patients with HCC. The ICC samples were taken from nine patients by surgical resection and six cadavers at autopsy, in addition to the sample used for SAGE. The characteristics of the patients are provided in Table 2. As samples of extrahepatic adenocarcinoma, we used BD Premium Total RNA™ (BD Biosciences Clontech, Palo Alto, CA) taken from adenocarcinomas of human breast (Cat. No.636635), colon (636634), stomach (636629), uterus (636628) and lung (636633).

The study protocol conformed to the ethical guidelines of the Declaration of Helsinki (1975). All patients provided written informed consent for the analysis of the biopsy specimens and the hospital ethics committee approved the study.

2.2. SAGE

Each tissue sample was homogenised in liquid nitrogen and total RNA was extracted using a ToTALLY RNA™ kit (Ambion, Austin, TX). The polyadenylated RNA (polyA-RNA) was subsequently purified using a MicroPoly(A)Pure™ kit (Ambion). Aliquots of polyA-RNA (3 μg) from each ICC and HCC sample were used for SAGE, as described previously [15–17]. The NL tissue and HCC cDNA libraries have also been described previously [16,17]. To compare liver cancer with cancers from other organs, we obtained 16 SAGE libraries from the National Center for Biotechnology Information (NCBI) SAGEmap (http://www.ncbi.nlm.nih.gov/SAGE/). These libraries originated from the tumours of the stomach (G189 and G234), colon (Tu98 and Tu102), prostate (PrCA-1 and Chen_Tumour_Pr) and breast (95-259, 95-347, DCIS, DCIS-2, DCIS-3, DCIS-4, DCIS-5, IDC-3, IDC-4 and IDC-5).

For the analysis of molecular functions, we used all databases registered in MetaCore™ from GeneGo Inc. (http://portal.genego.com/cgi/index.cgi). Statistical significance in this database was calculated using the basic equation (Supplementary Fig. 1).

2.3. Quantitative real-time RT-PCR detection

Template cDNA was synthesised from 1 μg of total RNA using SuperScript™ II RT (Invitrogen, San Diego, CA). The quantitative real-time RT-PCR detection was performed using a TaqMan® Gene Expression Assay kit (Applied Biosystems, Foster City, CA). The amount of glyceraldehyde-3-phosphate dehydrogenase (*GAPDH*) (Hs99999905) mRNA in each sample was used to standardise the quantity of each of the following mRNA: Cbp/p300-interacting transactivator with Glu/Asp-rich carboxy-terminal domain 4 (*CITED4*) (Hs00388363), glutathione-*S*-transferase pi (*GSTP1*) (Hs00168310), biglycan (*BGN*) (Hs00156076), insulin-like growth factor-binding protein 5 (*IGFBP5*) (Hs00181213), claudin-4 (*CLDN4*) (Hs00533616), phosphofructokinase platelet type (*PFKP*) (Hs00242993), transmembrane 4 L six family member 1 (*TM4SF1*) (Hs00371997), calpain 1 (mu/l) large subunit (*CAPN1*) (Hs00559804) and claudin-10 (*CLDN10*) (Hs00199599).

2.4. Immunoblot analysis

Each tissue sample was homogenised in liquid nitrogen and a protein extract was prepared using radioimmunoprecipitation assay (RIPA) buffer. The extracts (7 μg/lane) were subsequently electrophoresed on SDS–10% polyacrylamide gels and transferred onto polyvinylidene fluoride. An extract prepared from KMBC cells, a human extrahepatic bile duct carcinoma cell line [21], was used as a positive control. The blots were then incubated for 1 h with goat polyclonal antibodies against claudin-4 (1:200 dilution; Santa Cruz Biotechnol-

Table 1
Characteristics of the samples used for RT- PCR and SAGE

	NL $N = 7$	CLD $N = 20$	HCC $N = 26^a$	ICC $N = 16^a$
Mean age, years (SE)	64.6 (4.3)	62.7 (2.1)	65.0 (1.9)	67.9 (2.7)
Sex				
Female	3	5	6	5
Male	4	15	20	11
Hepatitis virus infection				
HBsAg-positive	0	8	9	
HCV-Ab-positive	0	12	16	
Mean ALT (SE) (IU/L)	14.2 (2.0)	61.3 (13.9)	52.6 (11.0)	47.0 (13.8)
Mean ALP (SE) (IU/L)	234.4 (36.2)	289.0 (33.1)	321.3 (31.5)	482.0 (87.1)
Mean GGT (SE) (IU/L)	93.3 (72.0)	88.0 (14.4)	82.9 (14.1)	185.5 (61.1)
Mean AFP (SE) (ng/mL)	NA	81.8 (29.7)	80.9 (24.6)	NA
Mean CEA (SE) (ng/mL)	NA	NA	5.3 (0.8)	20.9 (14.0)
Mean CA19-9 (SE) (U/L)	NA	NA	36.7 (3.7)	1171.5 (767.1)

NL, normal liver; CLD, chronic liver disease; HCC, hepatocellular carcinoma; ICC, intrahepatic cholangiocarcinoma; ALT, alanine aminotransferase; ALP, alkaline phosphatase; GGT, gamma-glutamyl transferase; AFP, alpha-foetoprotein; CEA, carcinoembryonic antigen; CA19-9, carbohydrate antigen 19-9; NA, not available.

[a] We used one ICC sample and three HCC samples for SAGE.

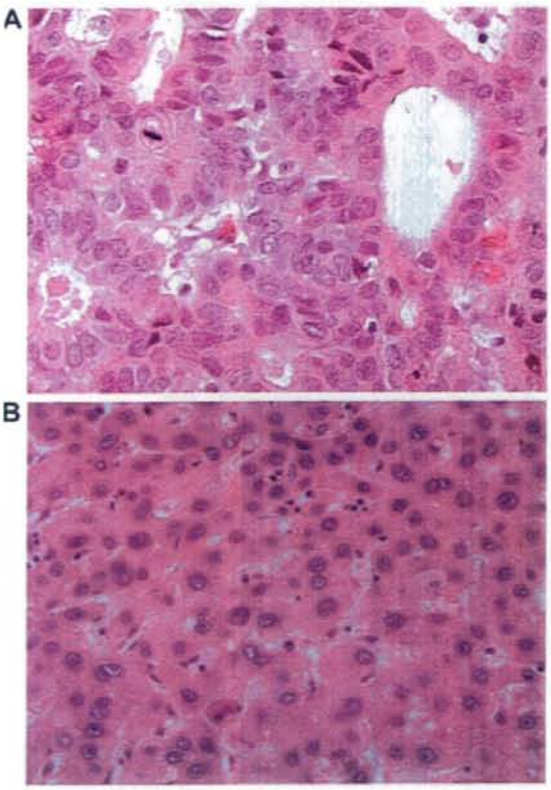

Fig. 1. Histopathological findings of the samples used for the serial analysis of gene expression. (A) Moderately differentiated intrahepatic cholangiocellular carcinoma. (B) Well-differentiated hepatocellular carcinoma. [This figure appears in colour on the web.]

ogy, Santa Cruz, CA). The blots were then washed and exposed to rabbit anti-goat IgG (1:1000 dilution) for 30 min and visualised using the ECL™ kit (GE Healthcare UK Ltd., Little Chalfont, UK).

2.5. Immunohistochemical analysis

For immunohistochemical analysis, we used 16 ICC samples and 16 HCC samples. Deparaffinised sections were treated with primary antibodies against CLDN4 (diluted 1:24, rabbit polyclonal antibodies; Cat. No. sc-17664; Santa Cruz Biotechnology) for 40 min at room temperature after appropriate antigen-retrieval treatment. Primary antibody/antigen binding was detected using a standard streptavidin–biotin–peroxidase technique (LSAB2 Kit Universal/HRP Rabbit/Mouse; DAKO, Glostrup, Denmark) and visualised using a DAB+ (3,3′-diaminobenzidine tetrahydrochloride) Liquid System (DAKO).

2.6. Discrimination analysis

We performed discrimination analysis based on the mRNA expression data using Dr. SPSS II software (SPSS Inc., Chicago, IL) to create an ICC classifier. Fifty-three of the seventy-four samples mentioned above were selected randomly: seven ICC, four NL, 20 CLD, 17 HCC and five extrahepatic adenocarcinoma samples. These 53 samples, which were subjected to RT-PCR analysis, were considered to be the training group. To verify the validity of the analysis, we performed RT-PCR using another 21 samples: nine ICC, three NL and nine HCC samples.

2.7. Statistical analyses

One-way ANOVA and Tukey–Kramer analyses were used for the statistical analysis of RT-PCR data.

3. Results

3.1. SAGE profiles of ICC

We obtained a total of 93,874 SAGE tags: 34,079 from the ICC library and 59,795 from the HCC library. Of these, 30,859 tags were unique: 14,168 and 16,689

Table 2
Clinicopathological features and discrimination analysis of the ICC samples used for RT-PCR

No.	Age (yr)	Gender	Virus	Tumour location	Size (cm)	Stage[a]	Gross appearance	Diff.	Serological marker		Z-Score	Predicted result[d]
									CEA[b] (ng/mL)	CA19-9[c] (IU/mL)		
ICC samples of the training group												
1	58	M	HCV	P	3.0 × 2.5	3	MF	Mod	5.20	23.00	4.02	ICC
2	73	M	HCV	A/P	6.5 × 5.5	4B	MF	Poor	NA	NA	7.09	ICC
3	72	M	No	A/P	7.0 × 6.5	4A	MF	Mod	7.50	NA	1.56	ICC
4	76	M	HBV	L/Med	5.3 × 4.7	4B	MF+PDI	Mod	46.00	8,600.00	2.16	ICC
5	68	F	HCV	A/P	9.0 × 6.0	4B	MF+PDI	Poor	NA	NA	0.56	ICC
6	65	M	HCV	Mu	4.0 × 3.0	4A	MF	Poor	0.00	87.00	1.31	ICC
7	53	M	HCV	Med	4.5 × 3.0	4A	PDI+MF	Poor	5.20	1,161.00	6.31	ICC
ICC samples of test group												
8	35	F	No	A/P	6.8 × 4.5	4A	MF + PDI	Poor	455.43	168.80	1.34	Not ICC
9	81	F	No	L	2.6 × 2.0	3	MF	Mod	164.58	5.10	1.63	ICC
10	73	M	No	P	5.0 × 4.0	3	MF	Mod	191,886.86	1.10	206.40	ICC
11	71	F	No	A/P	10.0 × 9.0	3	MF	Mod	3335.47	NA	13.28	ICC
12	72	F	No	M	5.0 × 4.5	3	PDI	Mod	28,614.09	NA	43.17	ICC
13	70	M	No	M	4.0 × 3.0	3	MF	Well	4533.44	4.10	16.17	ICC
14	61	M	HCV	P	1.8 × 1.5	3	MF	Mod	573.55	3.80	2.05	ICC
15	80	M	HCV	A/P	3.5 × 2.7	3	MF	Mod	2914.25	0.00	9.16	ICC
16	62	M	No	L/Med	5.2 × 3.7	3	MF	Mod	11,024.51	3.40	28.45	ICC

ICC, intrahepatic cholangiocarcinoma; Diff, differentiation; M, male; F, female; A, anterior segment; P, posterior segment; Med, medial segment; L, lateral segment; Mu, multiple segment; MF, mass-forming type; PDI, periductal infiltrating type; well, well differentiated; mod, moderately differentiated; poor, poorly differentiated.

[a] International Hepato–Pancreato–Biliary Association (IHBPA) classification [20].

[b] The normal range of CEA is <5 ng/mL.

[c] The normal range of CA19-9 is <37 IU/mL.

[d] The predicted results were determined using leave-one-out cross-validation.

tags from the ICC and HCC library, respectively. Scatterplots using all tags indicated that the ICC expression profile was different from that of HCC ($R = 0.4629$) and NL ($R = 0.3438$; Supplementary Fig. 2), whereas the HCC expression profiles were correlated with those of NL ($R = 0.8632$; data not shown). We also observed a strong correlation between the expression profile of the HCC used here and that of another HCC ($R = 0.8027$; data not shown) [17]. These findings suggest that the expression profile of ICC differed from those of HCC and NL.

To eliminate as much sequence error as possible, only tags with two or more hits were selected from the ICC library, resulting in 3707 tags. When we searched for these tags in the NCBI SAGEmap (http://www.ncbi.nlm.nih.gov/SAGE/), we found that 1348 (36.4%) corresponded to single known genes, 341 (9.2%) corresponded to single expressed sequence tags (EST) and 1740 (46.9%) had multiple matches. The remaining 278 tags (7.5%) did not correspond to any known gene.

3.2. Gene signatures of ICC

We compared the transcript abundance in the ICC and HCC libraries without excluding tags with one hit and found that the levels of expression of 1898 genes were enhanced over fivefold in ICC. As expected, several genes, previously reported to be upregulated in ICC, were amongst the 20 genes that showed the greatest degree of upregulation (Table 3), including *KRT7*, *KRT19* and *S100 calcium-binding protein A6* (*S100A6*) [22]. We also identified several genes not previously well characterised as associated with ICC, such as *BGN* and *IGFBP5*. Some of the ICC-specific genes were not detected in the NL library, suggesting that these gene signatures may be specific to cholangiocytes.

To determine the molecular functions of the 1898 genes that were overexpressed in ICC than in HCC, we analysed all the SAGE tags representing these genes in the MetaCore™ from GeneGo Inc. (Supplementary Table 2). The biological processes of these genes included the regulation of cell adhesion molecules, translation initiation and the regulation of wingless-type MMTV integration site (Wnt) signalling ($P < 0.01$; statistical significance calculated using the basic equation in Supplementary Fig. 1).

We also found that 702 genes were underexpressed over fivefold in ICC relative to HCC without excluding tags with one hit; the 20 genes that showed the greatest degree of downregulation in ICC are listed in Supplementary Table 3. Amongst these were genes encoding apolipoprotein, fibronectin and haptoglobin, which were also underexpressed in ICC relative to NL. The biological processes associated with these genes (Supplementary Table 4) included immune response and the

Table 3
Twenty genes overexpressed in ICC compared to HCC

SAGE Tag	RefSeq ID	Gene name	Tag count			Fold (ICC/HCC)
			ICC	HCC	NL	
GACGCCGAAC	NM_133467	Cbp/p300-interacting transactivator, with Glu/Asp-rich carboxy-terminal domain, 4	111	1	9	122.00
CCTGGTCCCA	NM_005556	Keratin 7	103	0	0	113.00
AATAGAAATT	NM_000582	Secreted phosphoprotein 1 (osteopontin, bone sialoprotein I, early T lymphocyte activation 1)	83	1	0	92.00
CCCCCTGGAT	NM_014624	S100A6 S100 calcium-binding-protein A6 (calcyclin)	66	0	0	73.00
CTTCCAGCTA	NM_004039	Annexin A2	55	1	3	61.00
GCAATCCTGT	NM_006998	Secretagogin, EF hand calcium-binding protein	52	0	0	58.00
GACATCAAGT	NM_002276	Keratin 19	50	0	0	55.00
GCAAAGAAAA	NM_006769	LIM domain only 4	44	0	3	49.00
CAGGCCCCAC	NM_005620	S100 calcium-binding protein A11 (calgizzarin)	41	1	0	46.00
GGAGACTTCC	NM_001153	Annexin A4	36	0	3	39.00
TGGCCCCACC	NM_002654	Pyruvate kinase, muscle	36	1	3	39.00
GCATTTGACA	NM_001046	Solute carrier family 12 (sodium/potassium/chloride transporters), member 2	33	0	0	36.00
AACTTGGCCA	NM_002423	Matrix metalloproteinase 7 (matrilysin, uterine)	30	1	0	33.00
AGGTCCTAGC	NM_000852	Glutathione-*S*-transferase pi	30	0	6	33.00
ATCTTTCTGG	NM_003406	Tyrosine 3-monooxygenase/tryptophan 5-monooxygenase activation protein, zeta polypeptide	30	1	0	33.00
TGATGTCTGG	NM_020182	Transmembrane, prostate androgen induced RNA	30	0	0	33.00
GACCGCAGGA	NM_001845	Collagen, type IV, alpha 1	27	1	0	30.00
GCCTGTCCCT	NM_001711	Biglycan	27	1	6	30.00
GGAACAAACA	NM_013230	CD24 molecule	27	0	0	30.00
TATGAATGCT		No reliable match	27	0	0	30.00

SAGE, serial analysis of gene expression; ICC, intrahepatic cholangiocarcinoma; HCC, hepatocellular carcinoma; NL, normal liver.

regulation of inflammation via complement activation ($P < 0.01$). These results suggest that the gene expression pattern of ICC is different from that of HCC.

Amongst the genes that were upregulated more than 20 times in the ICC library compared with the HCC library, we selected nine that were not previously well characterised to be overexpressed in ICC (Table 4) for further analysis. We defined these genes as the candidate markers of ICC and compared the SAGE libraries originating from extrahepatic adenocarcinoma (Supplementary Table 5). By comparing the mean transcript abundance in ICC with those in the other libraries, excluding tags with one hit, we found that eight genes (*CITED4*, *BGN*, *IGFBP5*, *CLDN4*, *PFKP*, *TM4SF1*, *CAPN1* and *CLDN10*) showed a threefold greater expression in ICC than in at least three other organs. These genes appear to be useful not only for the differentiation of ICC and HCC, but also for the differentiation of ICC and metastatic liver cancer.

3.3. RT-PCR and protein expression analyses

The above findings are based on the library analysis of one ICC sample; thus, their reliability must be validated with multiple samples. Moreover, the application of SAGE results to routine diagnostic examination is indispensable. We performed RT-PCR using RNA samples isolated from seven ICC, four NL, 20 CLD, 17 HCC and five extrahepatic adenocarcinomas (breast, colon, stomach, ovary and lung) to validate the expression data for the eight genes mentioned above. Of these eight genes, three (*BGN*, *IGFBP5* and *CLDN4*) were more highly expressed in ICC than in NL, CLD, HCC or extrahepatic adenocarcinomas ($P < 0.05$; Fig. 2; Supplementary Table 1), suggesting that these three genes are the specific gene signatures for ICC.

Of *BGN*, *IGFBP5* and *CLDN4*, the expression of CLDN4 was confirmed by immunoblotting (Fig. 3A) and immunohistochemical analyses (Fig. 3B and C). Immunoblotting revealed strong CLDN4 expression in six of seven patients with ICC and KMBC. In contrast, slight or no expression was detected in HCC and NL (Fig. 3A). Immunohistochemical analysis showed intense membrane staining in ICC, whereas no CLDN4 expression was observed in HCC (Fig. 3B and C).

3.4. Discrimination analysis

Based on the expression patterns of *BGN*, *IGFBP5* and *CLDN4* in the 53 samples of the training group, we performed discrimination analysis to obtain coefficients for these three genes, which were then used to

Table 4
Nine genes not previously well characterised and showing >20-fold overexpression from the ICC library compared to the HCC library

RefSeq ID	Gene name	Tag count		Ratio of RT-PCR					*P* value[a]
		ICC	HCC	ICC	NL	CLD	HCC	Other	
NM_133467	Cbp/p300-interacting transactivator, with Glu/Asp-rich carboxy-terminal domain, 4	122	1	27.56	1.37	1.81	1.13	0.13	0.0305
NM_000852	Glutathione-*S*-transferase pi	33	0	10.61	2.33	2.54	1.8	1.4	–
NM_001711	Biglycan	30	1	5.4	1.06	1.19	0.68	0.35	<0.0001
NM_000599	Insulin-like growth factor-binding protein 5	24	0	11.13	1.86	0.68	0.83	0.21	<0.0001
NM_001305	Claudin-4	24	1	344.98	1.71	7.92	8.56	0.44	0.0036
NM_002627	Phosphofructokinase, platelet	24	0	160.68	0.5	0.13	0.08	6.16	0.0089
NM_014220	Transmembrane 4 superfamily member 1	24	0	4,687.43	25.12	37.64	498.02	0.44	0.1882
NM_005186	Calpain 1, (μ/l) large subunit	21	1	4.32	1.33	0.92	0.85	5.76	<0.0001
NM_006984	Claudin-10	21	0	6.25	0.56	2.69	0.11	21.26	0.0638

ICC, intrahepatic cholangiocarcinoma; NL, normal liver; CLD, chronic liver disease; HCC, hepatocellular carcinoma; Other, extrahepatic adenocarcinoma; ICC, intrahepatic cholangiocarcinoma; HCC, hepatocellular carcinoma.
[a] One-way ANOVA.

define the *Z*-score as positive in ICC (Fig. 4A). The prediction performance of the discrimination analysis showed an efficient ROC curve (AUC = 0.987) (Fig. 4B). To verify the validity of this classifier, we calculated the *Z*-score for the 21 samples in the test group and found that the score was positive for all the ICC samples (Fig. 4C). Thus, we could distinguish ICC from the other cancers using this classifier.

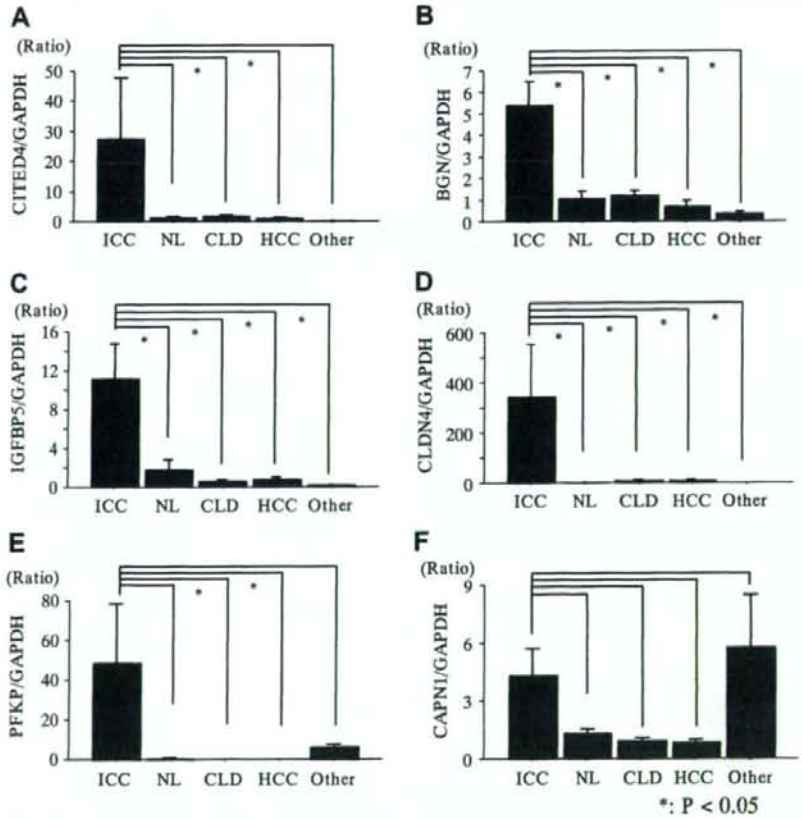

Fig. 2. Results of RT-PCR for intrahepatic cholangiocarcinoma (ICC), normal liver (NL), chronic liver disease (CLD), hepatocellular carcinoma (HCC) and other adenocarcinomas. GAPDH, glyceraldehyde-3-phosphate dehydrogenase; CITED4, Cbp/p300-interacting transactivator with Glu/Asp-rich carboxy-terminal domain 4; BGN, biglycan; IGFBP5, insulin-like growth factor-binding protein 5; CLDN4, claudin-4; PFKP, platelet-type phosphofructokinase; CAPN1, calpain 1 (μ/l) large subunit.